Iran J. Earth Sci. 2026; 18(1): 97-115

Iranian Journal of Earth Science (IJES)

https://doi.org/10.57647/j.ijes.2025.16895

Research Article

The Petrogenesis of Cretaceous Volcanic Rocks in the Northern Alborz According to Petrographic and Geochemical Studies

Rowshanak Arghaee[1,*], Mansour Ghorbani[1], José Francisco Santos[2]

[1]*Faculty of Earth Science, Shahid Beheshti University, Tehran, Iran*
[2]*Geobiotec, Department of Geosciences, University of Aveiro, Aveiro, Portugal*

[*]**Corresponding author:** arghaee.rk@gmail.com

Article History

Received:
22 September 2024
Revised:
24 October 2024
Accepted:
06 November 2024
Published online:
09 June 2025
Published in Issue:
31 March 2026

Abstract:
Cretaceous volcanic rocks are extensively developed in the Alborz structural zone, located in northern Iran. The petrogenesis and evolution of the northern Alborz basalts and other volcanic rocks have been studied before, but various theories have been proposed regarding their petrogenesis and geodynamic settings. To further explore their petrogenesis, we are conducting a study featuring three different regions of the northern Alborz dominated by extensive outcrops of Cretaceous volcanic rocks. The study area consists of the southern part of Amol city, JavaherDasht village in the east of Gilan province, and south of Lahijan in NarenjLengeh village in the west of Gilan province. Petrographic examination of the studied rocks shows evidence of primary magma, indicating the presence of alkaline magma in the region. Feldspathoids such as nepheline and nosean dominate most samples, providing evidence of alkaline magmatism. All analyzed samples from these three regions fall within the alkaline series. Geochemical studies point to a rift tectonic with significant crustal contamination. In a spider diagram of incompatible elements, an increase in the Nb/La ratio indicates crustal contamination, which is generally observed in continental rifts. All samples exhibit depletion of Y, confirming intraplate magmatism within the region. Chondrite-normalized rare-earth-element (REEs) patterns show a notable enrichment in light REEs (LREEs) relative to heavy REEs (HREEs). Our study suggests a rift tectonic setting for the northern Alborz rocks with prevalent alkaline magmatism during the Cretaceous.

Keywords: Northern Alborz; Alkaline magmatism; Continental rift; Crustal contamination

Cite this article: Arghaee R., Ghorbani M. & Santos J. F. (2026). "The Petrogenesis of Cretaceous Volcanic Rocks in the Northern Alborz According to Petrographic and Geochemical Studies." *Iranian Journal of Earth Science*, *18*(1), 97-115. https://doi.org/10.57647/j.ijes.2025.16895

1. Introduction

The studied areas are located in the northern Alborz, which is part of the Central Alborz zone. The dynamic evolution of the northern Alborz basalts and other volcanic rocks has been extensively studied, with various tectonic settings proposed. Some theories associate these basalts with ophiolite complexes (Arjmandzadeh et al., 2017; Kananian et al., 2004; Salavati, 2008; Salavati et al., 2009; Salavati & Samadissofi, 2008; Zaeimnia et al., 2008), while others suggest back-arc basins and supra-subduction zones (Akmali et al., 2019; Monsef et al., 2022; Rezaei et al., 2020; 2023; Vasigh et al., 2014; Verdel et al., 2011). However, most reports in our study areas indicate that Cretaceous volcanic rocks in the northern Alborz are characteristic of continental intraplate alkaline volcanism, spatially and temporally associated with extensional tectonics and rifting events (Abdi et al., 2014; Aghazadeh, 2002; Akmali, 2016; Amani et al., 2020; 2021; Arghaee, 2017; 2025; Arghaee & Ghorbani, 2021; 2022a; Dabiri et al., 2018b; Delavari et al., 2018; Doroozi et al., 2016; 2015; Haghani & Taki, 2012; Haghnazar, 2009; 2011; Haghnazar & Malakotian, 2009; Haghnazar et al., 2011; 2008a; 2015; 2016; 2008b; Jafari Sough et al., 2018;

Moradi, 2017; Nazari et al., 2023; Taki, 2017; Yazdi et al., 2016; 2022) In his PhD thesis, (Haghnazar, 2009) investigated JavaherDasht area basalts, finding isotopic ratios 143Nd/144Nd and 87Sr/86Sr, indicative of intra-continental rift magmatism. Additionally, some researchers posit that the abundant Late-Cretaceous volcanism in the northern Alborz may be linked to significant mantle thermal perturbations, potentially associated with asthenospheric upwelling and plume activity (Arghaee, 2017; 2024; Arghaee et al., 2024; Dabiri et al., 2018a; Delavari et al., 2018; Mollai et al., 2021; Namvar, 2018; Ousta et al., 2024).

Consequently, this study aims to bridge this knowledge gap to achieve a single goal in petrogenesis by investigating three distinct regions in the northern Alborz with extensive outcrops of Cretaceous volcanic rocks. Analyzing the chemical compositions and thin sections of these volcanic rocks serves as a crucial method for elucidating the connections between magma sources, eruptive processes, and plate tectonics in the area. 60 thin sections of Cretaceous basalts and associated volcanic rocks have been examined. Additionally, 24 samples of Cretaceous volcanic rocks in northern Alborz have been analyzed for major and trace elements using ICP-MS. This analysis aims to determine their origin and formation mechanism.

2. Materials and Methods

A total of 100 samples were selected from the Cretaceous basalts and associated volcanic rocks across three regions of the northern Alborz. These samples were collected from outcrops, with 60 designated for thin-section analysis. Some thin sections were examined at the University of Aveiro in Portugal, while others were analyzed at Shahid Beheshti University in Iran. Additionally, 24 whole-rock samples underwent ICP-MS analysis. The major oxide and trace elements data for these whole rocks were obtained at "Zarazma Mineral Studies Co. of Iran" using the MMS-01 (Rock) ICP-MS method (Table 1-Table 3).

3. Geological Background

The Alborz Mountain range extends from Azerbaijan in the northwest to Khorasan in the northeast (Jackson et al., 2002; Malaekeh et al., 2021; Zanchi et al., 2006; 2009). Alborz's structural zone is classified as Western, Central, and Eastern, which is limited to the west-central and eastern Alborz Mountains. The studied areas are located in the northern Alborz, which is part of the Central Alborz zone. This zone is the main part of the Alborz Mountains of northern Iran, determined as a part of the Alpine-Himalayan orogenic belt's northern margin (Ghasempour et al., 2014; Malaekeh et al., 2021; Zanchi et al., 2006).

The Alborz Mountains as the main section of the Alborz structural zone have an important role in metallic ore mineralization. It hosts many Pb, Zn, Ba, Fe, and rare earth elements (REE) ore deposits (Malaekeh et al., 2021; Rajabi et al., 2013). In the Central Alborz, there are two types of mineralization: epigenetic mineralization hosted in Triassic rocks (Elika Formation) or Permian rocks (Ruteh Formation)(Ghorbani, 2013). Given that the mineralization is epigenetic, it is younger than the host rocks, forming high-grade veins within them. As both mineralization types are epithermal, it is likely that these epithermal solutions are associated with Cretaceous volcanism (basalts of the studied area), since there has been no recorded volcanism in the Central Alborz zone during the Cenozoic or any period post-Triassic other than the Cretaceous.

Comprising mainly platform-type lithofacies from the Neoproterozoic to Quaternary periods, the Alborz range is bordered by the Caspian depression in the north and Central Iran in the south (Ghorbani, 2021). During the Ordovician to Silurian periods, the Alborz separated from Gondwana and finally collided with the Eurasia plate in the Triassic (Alavi, 1991; Stampfli, 1996). Therefore, the Alborz can be considered an active mountain belt, resulting from the Gondwana and Eurasia plate collision in the Triassic (Berberian & King, 1981; Guest et al., 2006; Sengor, 1990; Sengor et al., 1988; Stampfli et al., 1991; Stocklin, 1974a). The Alborz is characterized by the dominance of platform-type sediments, including limestone, and clastic rocks. Rock units from Precambrian to Quaternary have been identified, with some hiatuses and unconformities in the Paleozoic and Mesozoic (Ghorbani, 2013). In the early Mesozoic, carbonate sediments were deposited in the central and the northern Alborz followed by the Shemshak Formation in the late Triassic (Berberian et al., 1982; Nazari et al., 2004). Volcanic activity during the Paleozoic and early Mesozoic was minimal (Stocklin, 1974b); however, upper Cretaceous volcanic rocks are widespread in the northern Alborz (Aghanabati, 2004). Notably, significant submarine volcanic eruptions occurred locally in the northern Alborz during the Cretaceous period (Arghaee, 2024; Arghaee et al., 2024; Moradi, 2017; Stocklin, 1974b), including basaltic eruptions in the late Cretaceous (Akmali, 2016; Allen et al., 2003; Delavari et al., 2018; Haghnazar, 2012; Moradi, 2017).

3.1 Geological Setting

Cretaceous volcanic rocks are extensively developed in two structural zones of Iran: the Sanandaj-Sirjan structural zone (Khan Nasr Esfahani, 2012) and the Alborz structural zone in the north of Iran (Ghorbani, 2021) The study samples are situated within the Alborz structural zone (Figure 1(a)). This article will examine three different regions in the northern Alborz, each with significant outcrops of Cretaceous volcanic rocks. The three study areas are as follows (Figure 1(a)):

1) The Cretaceous basalts and associated volcanic rocks south of Amol, located 20 kilometers to the southern part of the city on the Amol geological map (Vahdati Daneshmand, 1991) (Figure 1(b)). A part of the sandstone and shale of the Shemshak formation (Lower Jurassic) could be seen after the

10.57647/j.ijes.2025.16895

Siah-Bisheh tunnel in the region. Generally, the Cretaceous basaltic and trachytic lavas that we studied were placed on the top of this formation. The basaltic lavas collected from this area, are located in the deposits of the Tizkoh formation and belong to the Early Cretaceous.

2) The basalts in the JavaherDasht area (a village in Siahkalrud Rural District) with extensive outcrops in the northern part of the Alborz mountains, east of Gilan province, depicted on the Javaherdeh map (Baharfiruzi & Shafeii, 2003) (Figure 1(c)). Cretaceous basalts in this region are generally observed along the river and on the Shemshak formation.

3) The volcanic rocks in the south of Lahijan in NarenjLengeh village, west of Gilan province in the northern Alborz, marked on the Qazvin-Rasht geological map (Annells et al., 1975) (Figure 1(d)). The basaltic lavas collected from this area are placed on the deposits of the Tizkoh formation, which clearly shows the characteristics of the marine environment.

4. Results

4.1 Petrography

4.1.1 *South of Amol*

The diversity of rocks observed in thin sections from the south of the Amol region, based on petrographic and geochemical data, includes AlkaliBasalts (Basanite, Tephrite), Trachybasalt, Trachyte, Phonolite, and Diabase.

In most studied trachyte thin sections, a microlitic texture is prevalent, with microlites typically oriented in one direction (Johannsen, 1931), suggesting lava flow on the surface. Trachybasalts exhibit a fine-grained texture without phenocrysts, indicating rapid eruption and a lack of residence in a magma chamber. In contrast, trachytes show a trachytic texture with abundant phenocrysts, implying a longer residence time in a magma chamber (Figure 2(a)). Plagioclase in trachytes is subhedral and exhibits corrosion, possibly due to increased magma temperature from lava flows in the Amol area.

Basanite samples display an amygdaloidal texture, with cavities filled by calcite and iron oxide. In basanites, olivine and pyroxene have altered to iddingsite, a process initiated at the crystal rim and progressing inward, likely due to high magma temperatures and increased oxygen fugacity (Figure 2(b)) (Middlemost, 1972).

Phonolites in Amol are green in hand specimens and emit a bell-like sound when struck, indicative of phonolites (Nelson & Montana, 1992). They have a microlitic texture with calcite-filled amygdaloids prevalent in the samples. Some plagioclase in these phonolites exhibits sieve texture, characterized by numerous small inclusions and a spongy appearance, which develops during decompression.

Diabases in this region show diabasic and intersertal textures with plagioclase phenocrysts surrounded by clinopyroxene and green chlorite. Plagioclase has altered to saussurite, pyroxenes to chlorite, and most olivine phenocrysts have altered to iddingsite.

4.1.2 *JavaherDasht*

Rocks in the thin sections from the JavaherDasht region, as determined by petrographic and geochemical data, include Basalt, Tephrite, Hawaiite, Gabbro, Trachybasalt, and Tuff.

Basalts in JavaherDasht contain clinopyroxene, plagioclase, and olivine, with epidote present as a secondary mineral from plagioclase alteration. The prevalent texture is porphyritic, with microlites and glass, and idiomorphic phenocrysts of clinopyroxene and olivine (Figure 2(c)). Some pyroxenes exhibit a purple-brown outer rim due to Al and Ti enrichment from pressure reduction and depth.

Tephrites show a trachytic texture, with a partially flowing matrix and fine-grained nepheline. Comb texture is present in sample Jd5, characterized by skeletal plagioclase and parallel needle-shaped clinopyroxene crystals. Nosean is found in some alkali basalts (Figure 2(d)), indicating an alkaline parent magma.

Hawaiite and trachybasalt share similar characteristics, with trachytic texture prevailing. Some trachybasalt samples contain amygdaloids filled with zeolite (Figure 2(e)).

The gabbro samples from JavaherDasht exhibit an intergranular texture with spaces between plagioclase crystals. Haghnazar (Haghnazar, 2012; Haghnazar et al., 2011) suggests that these gabbros, which are Cretaceous in age, share an origin with the basalts in the area.

The tuff matrix in this region primarily consists of flow microlites of sanidine and glass, indicative of a rapid and explosive release of rhyolites in the southern part of the study area (Haghnazar, 2009).

4.1.3 *South of Lahijan in NarenjLengeh village*

The thin section samples from the south of Lahijan in NarenjLengeh village, based on petrographic and geochemical data, include Alkali basalt (Basanite), Basaltic trachyandesites, Amygdaloidal Basanite, Pillow Basalt, Hawaiite, Basaltic andesites, and Lamprophyre.

In this region in basaltic trachyandesites, the predominant textures are trachytic or microlitic. Rapid eruption and cooling prevented complete phenocryst formation (Figure 2(f)). Automorphic clinopyroxene, often converted to iron oxide, is present. Increased iron oxide suggests high oxygen levels in the magma, while the absence of phenocrysts indicates rapid magma ejection at high temperatures. These samples exhibit extensive alteration with secondary carbonate and chlorite mineralization (Figure 2(f)). Epidote appears as a secondary mineral from plagioclase alteration. High magma temperatures and increased oxygen have altered olivine and pyroxene in basaltic trachyandesites to iddingsite (a red pseudo mineral containing trivalent iron oxide) (Morse, 1980).

The dominant texture of alkali basalts (basanite) in

10.57647/j.ijes.2025.16895

this region is an intersertal texture. The space between the plagioclase crystals is filled by the secondary minerals chlorite and calcite in these samples. In this matrix, pyroxene minerals with different interference colors, especially purple (purple clinopyroxene, indicative of titanaugite), and olivine can be seen. Most of the basanite samples are filled with the secondary mineral calcite, which may be responsible for resistance in the magma chamber. In the alkali basalts, a glomeroporphyritic texture is observed, indicating the accumulation of some phenocrysts such as pyroxene and plagioclase, which could be signs of crystal fractionation. Additionally, nosean, which can be evidence of alkaline magma, is present in the basanite samples from NarenjLengeh (Figure 2(h)).

In vesicular basanite in this area, the texture is similar to other basalts in this region, but this sample has many vesicles. These vesicles generally contain the secondary mineral (Bucher & Grapes, 2011) chlorite, which is dominant in some marine basalt (Figure 2(g)).

The pillow basalt core taken from this section revealed interesting points. The difference between the core of pillow lava and its shell is mainly related to the amount of gas bubbles present (Juteau & Maury, 1999). The pillows in this region have a distinct and coherent core that crystallizes without bubbles, indicating a low presence of gas bubbles. Basaltic pillows formed at great ocean depths have fewer and smaller cavities compared to those formed at shallower depths, or they may lack them altogether, even though the total amount of volatile substances in the magma that forms both types of lavas is the same (Best, 2003). It appears that, considering the absence of vesicles in our pillow samples, the water depth was not very shallow, suggesting that these pillow lavas flowed in deep water. The dominant texture of pillow basalts in the region is intersertal, where plagioclases intersect, and the irregular spaces between them are filled with pyroxene and olivine minerals (Figure 2(i)). The samples contain a high amount of secondary carbonate, and propylitic alteration observed as an indicator. Magmatic or hydrothermal solutions rich in magnesium, iron, calcium, sodium, or bicarbonate cause the formation of minerals such as epidote, chlorite, zoisite, or albite in igneous rocks.

Hawaiites in this region contain sanidine feldspar and exhibit a trachytic texture.

The presence of kaersutite, a common amphibole in alkaline intermediate rocks, is one of the important characteristics of lamprophyres in NarenjLengeh (Arghaee & Ghorbani, 2022b). Kaersutite forms elongated prisms with axes that mineralize with delays. Idiomorphic crystals, which have less surface area, are more stable. In a fully equilibrated state, a crystal is allowed to grow unrestrictedly in all dimensions. Most amphibole crystals in our samples appear to have reached this stable condition, indicating a slow growth rate (Best, 2003). Biotite is also clearly visible in these rocks. The potential petrogenesis of lamprophyre in the region is thought to be derived from hydrous basanitic or tephrite magmas, which have evolved in crustal dome regions and may have been emplaced during the early stages of continental rifting.

4.2 Geochemical Study

24 whole-rock samples were analyzed using the ICP-MS method and the major and trace element compositions are presented in Table 1-Table 3.

The volcanic rock samples were classified based on the SiO_2 vs. $K_2O + Na_2O$ classification diagram (TAS) by Le Bas (Le Bas et al., 1986) as trachybasalt, basaltic trachyandesites, basaltic andesites, phonotephrites, trachytes, alkali basalt, and basalt (Figure 3(a)). Although numerous diagrams were studied (Arghaee, 2025), not all are included here; however, they consistently indicate alkaline series magmatism, as evidenced in the TAS diagram (Figure 3(a)).

In the Na_2O vs. K_2O diagram (Figure 3(b)) (Wilson et al., 1995), the samples from the three regions were all in the alkaline-sodic series (Similar changes have been observed in the Alasht basalts of the northern Alborz (Arian et al., 2016), except for the Amol trachytes. It seems that crustal contamination caused an increase in K in these Amol samples, leading them towards the potassic series. In continental crust, increased crustal contamination causes a rise in K_2O. The sodic series evolves through hawaiite or nepheline-hawaiite, mugearite to trachyte or phonolite, such as our region (Philpotts & Ague, 2009).

4.2.1 *Examining the incompatible elements diagrams (Spider Diagram)*

4.2.1.1 *South of Amol*

Trachyte (SA4-SA14-SA15): The enrichment of Ta and Nb in trachytes of Amol, (Figure 3(c)) suggests a derivation from an enriched mantle source. The absence of a sharp negative anomaly in these two elements in Amol is characteristic of continental intraplate (Ballever et al., 2001).

The positive peak in Rb concentration may result from high absorption by plagioclase, or it could reflect a compensatory increase in Rb or because of fractional crystallization (Chatterjee & Bhattacharji, 2008). Alternatively, it might be due to Rb being one of the incompatible elements typically observed in continental rifts, possibly arising from crustal contamination (Ballever et al., 2001).

Depletion of Sr in the trachyte of Amol could be attributed to two reasons: 1) its mantle origin, and 2) the high mobility of Sr due to the alkaline nature of the primary magma, which is related to the crystallization of plagioclase (Rollinson & Pease, 2021). Trachyte exhibits more depletion of Sr compared to the alkali basalts of Amol, suggesting that the process of crustal contamination in trachytes was more significant than in alkali basalts, possibly due to their longer residence time in the magma chamber. Additionally, Sr depletion might be associated with the fractional crystallization of feldspars in continental rifts (Lan et al., 2022).

The depletion of Ti in the mantle likely occurred dur-

10.57647/j.ijes.2025.16895

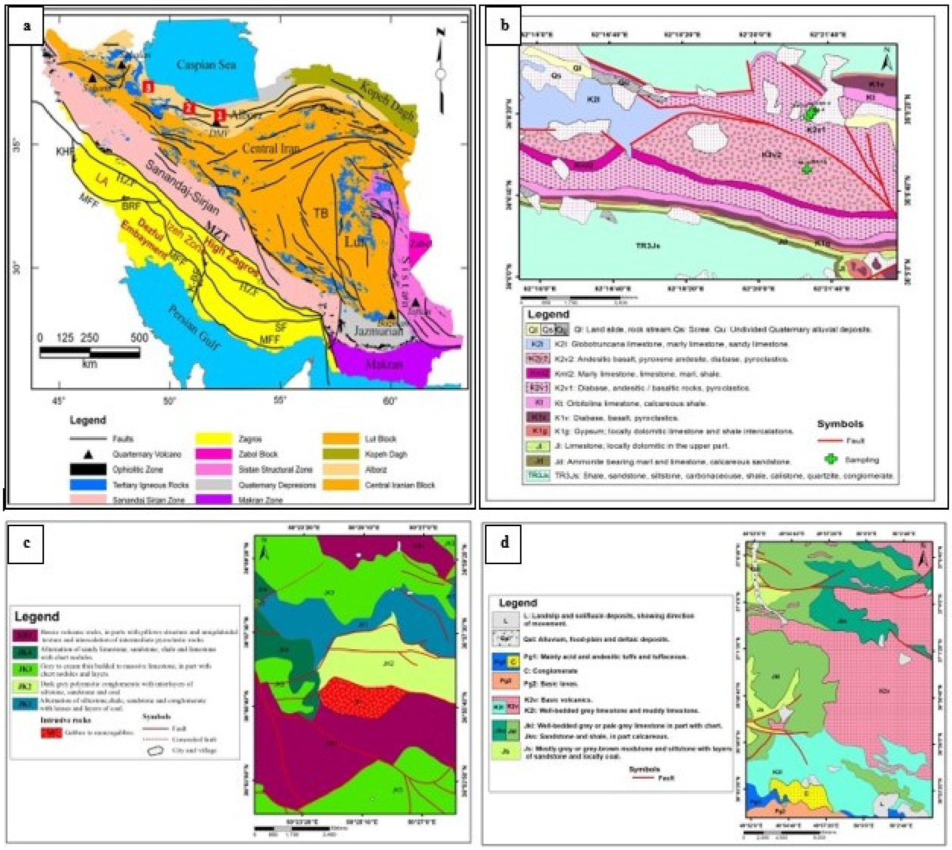

Figure 1. (a) Location of the studied area (1,2,3) on the simplified structural map of Iran (modified from the structural map of the National Geoscience Database of Iran, NGDIR; http://www.ngdir.ir modified by (Teknik & Ghods, 2017)) (b) The Cretaceous basalts and associated volcanic rocks in the simplified geological map of the South of Amol (1) (Based on the Amol 1:250,000 geological map by (Vahdati Daneshmand, 1991)) (c) Basaltic rocks in the JavaherDasht region (2). Simplified geological map of JavaherDasht (Based on the Javaherdeh 1:100,000 geological map by (Baharfiruzi & Shafeii, 2003)) (d) Simplified geological map of the South of Lahijan (3) (modified from the 1:250,000 geological map of Ghazvin-Rasht by (Annells et al., 1975))

Table 1. Whole-rock major oxide data (in wt%) for basaltic and trachyte rocks in the study area

Sample	SiO2	Al2O3	BaO	CaO	Fe2O3	K2O	MgO	MnO	Na2O	P2O5	SO3	TiO2	LOI	SrO
Jd-1	46.79	18.00	0.07	7.25	10.23	2.80	5.87	0.15	2.89	0.26	0.06	1.38	4.17	0.09
Jd-2	47.08	17.49	<	8.60	13.37	1.54	4.17	0.15	4.04	0.26	1.23	1.54	0.54	<
Jd-5	46.49	15.76	0.06	9.50	12.42	2.08	6.73	0.20	2.55	0.26	<	1.28	2.59	0.08
Jd-6	50.77	15.00	0.10	7.29	10.88	2.10	5.67	0.22	4.46	0.28	<	1.19	1.96	0.07
Jd-8	45.94	15.87	<	9.87	12.10	1.80	5.85	0.19	3.03	0.31	<	1.34	3.64	0.07
Jd-10	48.22	15.49	0.07	10.21	11.31	2.37	5.55	0.16	2.89	0.25	<	1.19	2.20	0.09
Jd-12	48.79	17.76	0.05	8.54	9.33	1.70	3.34	0.17	3.44	0.24	<	1.23	5.30	0.12
Jd-13	46.31	15.69	<	8.17	9.65	1.19	5.51	0.16	3.33	0.22	<	1.14	8.53	0.09
SA-1	52.22	16.03	0.05	3.38	11.67	1.29	2.19	0.13	6.86	0.89	<	2.48	2.80	<
SA-2	44.61	14.89	<	6.22	15.15	1.38	1.79	0.21	6.51	0.53	<	3.30	5.41	<
SA-4	59.71	17.56	<	1.73	6.26	4.97	0.39	0.14	6.35	0.06	<	0.50	2.28	<
SA-12	48.31	16.00	0.05	6.95	9.88	1.53	1.70	0.17	6.51	0.87	<	2.39	5.65	<
SA-14	60.27	16.90	<	0.82	7.73	5.94	0.17	0.24	5.81	<	<	0.40	1.59	<
SA-15	60.22	16.86	<	0.23	9.12	6.94	0.10	0.13	5.12	<	<	0.46	0.73	<
NL-1	51.45	15.08	0.05	6.10	8.63	2.21	3.91	0.14	4.23	0.22	0.09	1.05	6.83	<
NL-4	47.01	14.80	0.15	8.51	11.70	1.47	5.68	0.17	4.36	0.40	0.36	2.50	2.83	0.07
NL-5	46.21	14.67	0.15	9.08	11.94	0.83	5.88	0.15	4.29	0.36	0.34	2.58	3.45	0.07
NL-7	48.53	13.93	0.08	7.29	11.39	1.21	6.10	0.15	4.85	0.31	0.27	2.45	3.39	0.07
NL-8	45.42	14.33	<	9.26	12.17	1.17	5.64	0.20	4.27	0.40	0.26	2.75	4.02	0.09
NL-13	28.06	11.22	<	17.32	12.95	0.42	7.15	0.93	1.39	0.59	0.31	2.32	17.15	0.07
NL-14	30.51	12.13	<	17.16	11.65	0.53	6.83	0.82	1.71	0.66	0.31	2.51	15.00	0.08
NL-15	44.94	13.83	<	8.83	12.94	1.20	6.54	0.13	2.78	0.56	0.29	3.70	4.19	0.07
NL-18	50.16	14.14	0.05	7.50	10.28	1.34	4.78	0.08	3.27	0.59	<	2.94	4.77	0.10
NL-20	49.83	14.12	0.05	7.47	10.83	1.12	4.39	0.10	3.22	0.57	0.08	2.92	5.18	0.10

10.57647/j.ijes.2025.16895

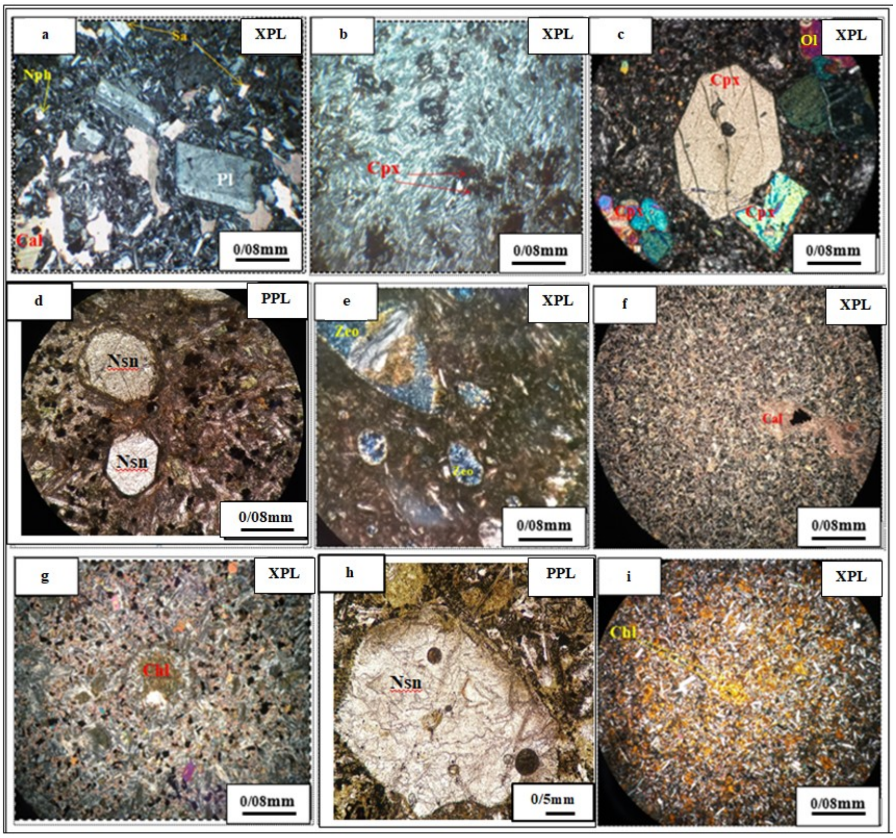

Figure 2. (a) Nepheline and sanidine in the trachytes of Amol (b) Iddingsite in the tephrite matrix of Amol (only we can see a trace of clinopyroxene) (c) Idiomorphic clinopyroxene observed in the basalt of a JavaherDasht sample (d) Nosean in tephrite from the JavaherDasht region (e) Amygdules filled with secondary zeolite in trachybasalt of JavaherDasht (f) Microlitic texture in trachybasalt from south of Lahijan (NarenjLengeh) (sample NL1) (g) Amygdaloidal basanite from NarenjLengeh filled with carbonate and chlorite (h) In PPL, nosean crystal with alteration develops along fracture planes. The difference in relief between the nosean remains and the alteration minerals are observed (i) Intersertal texture is the dominant texture of pillow basalts in the NarenjLengeh region where plagioclase intersects and the irregular spaces between them are filled with clinopyroxene and olivine minerals. Strong propylitic alteration, characteristic of secondary chlorites, is evident in this sample

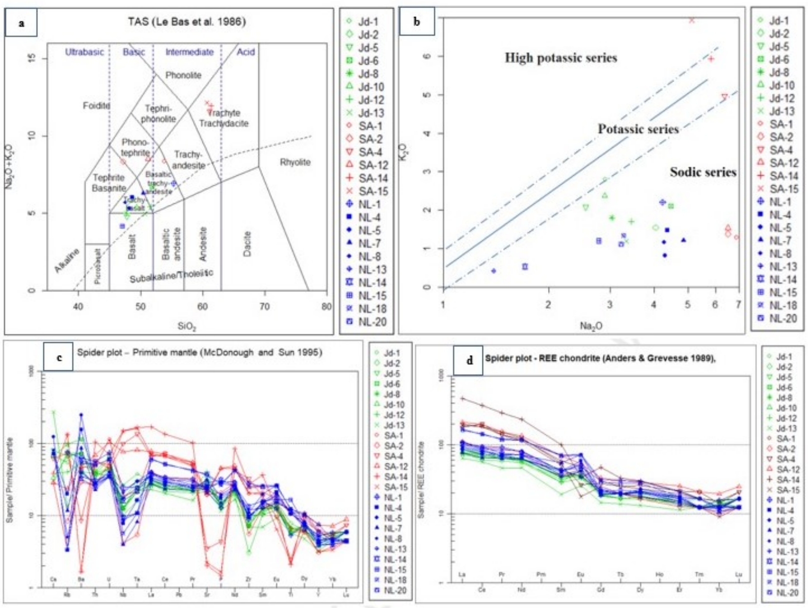

Figure 3. (a) SiO_2 vs. $K_2O + Na_2O$ classification (TAS) diagram of Cretaceous basalts and associated volcanic rocks in the three studied areas (Le Bas et al., 1986) (b) Differentiation of potassic series from sodic series (Wilson et al., 1995) (c) Spider diagram illustrating the distribution of incompatible elements in the studied areas (McDonough & Sun, 1995) (d) Chondrite normalized rare-earth-element (REE) plots for the volcanic rock samples from the northern Alborz (Anders & Grevesse, 1989)

10.57647/j.ijes.2025.16895

Table 2. Whole-rock trace and major element data (in ppm) for basaltic and trachyte rocks in the study area

Sample	Ag	Al	As	Ba	Be	Bi	Ca	Cd	Ce	Co	Cr	Cs	Cu	Dy
Jd-1	0.1	94881	4.4	476	1.3	<0.1	40447	0.1	43	26	33	0.6	58	4.2
Jd-2	0.2	91174	6.6	260	1.5	<0.1	47302	0.1	36	51.4	15	1.4	297	4.2
Jd-5	0.1	84852	1.8	472	1.4	<0.1	53799	0.1	43	37.2	51	1.7	83	4.2
Jd-6	0.3	79016	1.9	754	1.7	<0.1	41037	0.1	39	25.9	44	1.4	1	4.9
Jd-8	0.2	81575	1.9	267	1.5	<0.1	55220	0.1	40	34.3	72	<0.5	119	4.8
Jd-10	0.2	80075	1.1	491	1.4	<0.1	57164	0.1	42	34.9	89	0.7	158	4.3
Jd-12	0.3	90519	0.8	344	1.4	<0.1	46130	0.1	46	21.4	15	0.8	56	3.9
Jd-13	0.1	82439	3.1	235	1.2	<0.1	46058	0.1	34	30.7	75	5.7	39	3.2
SA-1	0.8	78666	3.9	311	1.9	<0.1	18932	0.1	111	21.6	68	0.6	7	5.6
SA-2	0.4	77480	0.5	192	1.8	<0.1	34773	0.1	55	36.7	9	<0.5	11	4
SA-4	1.2	75356	5.1	56	3.7	<0.1	9533	0.1	121	2.2	9	1.3	8	6.2
SA-12	0.8	80524	7.3	313	1.7	<0.1	38683	0.1	119	18.8	12	0.6	25	6.9
SA-14	1.1	79194	10	11	4.5	<0.1	4743	0.1	226	2.4	13	0.8	18	7.3
SA-15	0.7	73867	5.6	11	3.7	<0.1	1400	0.1	111	3	16	<0.5	174	4.2
NL-1	0.3	82808	2.8	415	1.6	<0.1	34669	0.1	57	23.3	22	<0.5	30	5
NL-4	0.6	76427	4.8	1032	1.2	<0.1	46555	0.1	44	34.9	132	1.5	85	5
NL-5	0.4	78265	1.8	1641	1.2	<0.1	50650	0.1	48	35	164	2.6	71	5.5
NL-7	0.5	75064	2.8	568	1.3	<0.1	41412	0.2	39	37.3	117	1.5	78	5.2
NL-8	0.5	74178	4.2	256	1.3	<0.1	50399	0.1	49	34.5	138	1.7	85	4.8
NL-13	0.6	58207	42.4	226	1.3	<0.1	95701	0.2	52	68.6	373	<0.5	72	5.1
NL-14	0.8	61288	11.6	214	1.3	<0.1	92703	0.1	51	63.2	297	<0.5	75	4.4
NL-15	0.5	70081	0.6	276	1.3	<0.1	48420	0.2	56	40.2	55	<0.5	27	5.1
NL-18	0.5	74046	2.5	354	2.3	<0.1	41787	0.1	85	31.4	107	<0.5	42	7.1
NL-20	0.8	73565	<0.5	384	2.2	<0.1	41789	0.1	87	27.8	114	<0.5	33	6.7

Sample	Er	Eu	Fe	Gd	Hf	In	K	La	Li	Lu	Mg	Mn	Mo	Na
Jd-1	2.1	2.08	58189	3.57	3.3	<0.5	22880	19	42	0.4	>2%	1056	0.5	19448
Jd-2	2.5	2.42	74239	3.66	1.5	<0.5	13219	18	20	0.4	17686	1058	1.1	27465
Jd-5	2.4	2.07	69864	3.8	2.9	<0.5	16736	20	12	0.3	>2%	1506	<0.5	17811
Jd-6	2.7	1.94	61273	3.96	3.2	<0.5	17463	17	38	0.4	>2%	1625	0.5	29957
Jd-8	2.8	1.87	66235	3.83	3	<0.5	15101	18	22	0.4	>2%	1340	<0.5	20550
Jd-10	2.3	2.04	63709	3.79	2.9	<0.5	19460	18	7	0.3	>2%	1132	<0.5	19940
Jd-12	2.3	1.82	52649	3.51	3.4	<0.5	13704	20	6	0.4	14367	1209	<0.5	22618
Jd-13	1.8	1.43	55414	2.84	2.8	<0.5	9722	15	6	0.3	>2%	1165	0.6	22940
SA-1	3.1	2.65	64890	5.88	5.6	<0.5	10557	47	13	0.5	10810	978	<0.5	45469
SA-2	2	2.28	76649	4.16	2.3	<0.5	11502	26	11	0.3	8894	1533	<0.5	44112
SA-4	3.4	1.47	36499	5.39	9.1	<0.5	38616	42	5	0.5	1802	1030	2.7	39992
SA-12	4	2.98	56444	6.49	6.7	<0.5	12822	50	9	0.6	8413	1289	1	43256
SA-14	3.4	1.89	45286	9.27	7	<0.5	45487	110	2	0.4	930	1750	1.6	35873
SA-15	2.3	0.99	52489	4.88	5.9	<0.5	49968	45	3	0.3	469	919	1.4	31970
NL-1	2.7	1.94	52754	4.26	3.2	<0.5	19250	25	37	0.4	17452	1086	<0.5	29448
NL-4	2.6	3.27	64814	3.96	3.6	<0.5	11979	20	22	0.4	>2%	1152	0.6	29179
NL-5	2.8	4.04	67604	4.16	4	<0.5	7641	21	47	0.4	>2%	1112	0.8	30214
NL-7	2.8	3.02	65475	3.76	3.4	<0.5	10501	18	28	0.3	>2%	1115	<0.5	34246
NL-8	2.4	2.3	67191	3.75	4.2	<0.5	9788	22	21	0.3	>2%	1449	0.5	28883
NL-13	2.6	2.79	69250	4.5	3.8	<0.5	3653	26	60	0.3	>2%	6306	<0.5	10050
NL-14	2.2	2.43	61449	3.69	3.4	<0.5	4500	24	41	0.3	>2%	5445	1.2	11842
NL-15	2.4	2.55	69946	4.15	4.5	<0.5	9997	24	13	0.3	>2%	964	0.7	19423
NL-18	3.3	4.02	59090	6.09	6.7	<0.5	11290	40	10	0.4	19701	593	0.9	22582
NL-20	2.8	3.91	61513	5.65	8.1	<0.5	9442	38	11	0.3	18551	739	1.3	22436

10.57647/j.ijes.2025.16895

Table 3. (Continued) Whole-rock trace and major element data (in ppm) for basaltic and trachyte rocks in the study area

Sample	Nb	Nd	Ni	P	Pb	Pr	Rb	S	Sb	Sc	Se	Sm	Sn	Sr
Jd-1	17.5	25.4	18	1279	<1	5.74	45	309	<0.5	19.5	<0.5	4.6	1	606.8
Jd-2	11	24.6	20	1153	1	5.22	33	4822	0.5	21.6	<0.5	4.2	2.2	416.7
Jd-5	8.4	27.6	26	1235	<1	5.56	40	214	3.4	28.8	<0.5	5.1	0.4	561.2
Jd-6	8.4	28.1	41	1296	<1	6.01	58	100	1.4	22.2	<0.5	6.4	1.1	492.4
Jd-8	8.1	28	46	1407	<1	5.74	47	260	6.2	23	<0.5	5.2	0.7	502.2
Jd-10	8.3	28.2	32	1163	8	5.77	40	148	14.2	25.4	<0.5	4.9	1.2	621.1
Jd-12	6.6	26.6	10	1249	2	5.68	24	65	4.7	17	<0.5	4.2	0.7	803.2
Jd-13	7.8	21	19	1046	<1	4.1	8	92	<0.5	25.3	<0.5	2.8	0.8	657.2
SA-1	12.4	55.6	7	4037	1	12.32	2	<50	<0.5	10.6	<0.5	8.5	2.2	388.5
SA-2	2.7	35.5	16	1854	6	7.91	5	68	<0.5	14	<0.5	5.2	0.7	385.6
SA-4	65	52.4	5	389	2	12.41	44	216	0.5	3	<0.5	7.5	2.7	69.1
SA-12	50.4	60.7	16	4075	3	13.82	14	114	0.6	10.3	<0.5	10.1	3.1	406.7
SA-14	98.1	105.6	4	132	8	25.78	79	60	<0.5	1	<0.5	14.8	6.2	40
SA-15	96.6	57	6	147	8	13.59	80	68	3.8	1.2	<0.5	7.9	5.1	43.9
NL-1	16.3	35.6	11	1163	3	8.26	45	697	3.5	19.6	<0.5	6.2	1.3	427.3
NL-4	5.1	28.6	55	1553	3	6.2	12	1371	3.3	22.2	<0.5	6.2	0.8	458.9
NL-5	5.7	32.1	59	1746	9	6.45	2	1307	18.1	22.4	<0.5	8	1.2	503
NL-7	2.6	28.2	58	1331	<1	5.6	7	753	54.8	23.9	<0.5	5.9	1	466
NL-8	13.5	29	67	1676	<1	5.98	3	1125	11.6	22.1	<0.5	5	1.2	626.3
NL-13	14.5	36.8	279	2617	<1	7.55	<1	1360	6.2	20.6	<0.5	6.2	0.8	463.7
NL-14	10.5	32.1	270	2820	<1	6.38	<1	1443	0.9	19.6	<0.5	5.4	0.7	557.6
NL-15	11.4	32	46	2547	1	6.76	<1	1637	<0.5	20	<0.5	6.4	1.7	506.1
NL-18	3.7	52.8	123	2382	<1	10.89	<1	236	<0.5	13.8	<0.5	10.5	2.4	711.8
NL-20	6.3	53.2	68	2489	1	10.52	2	269	<0.5	13.8	<0.5	10.1	2.6	754.3

Sample	Ta	Tb	Te	Th	Ti	Tl	Tm	U	V	W	Y	Yb	Zn	Zr
Jd-1	1.4	0.6	<0.5	2.7	8138	0.2	0.3	0.9	217	<1	15.6	2.03	76	92
Jd-2	1.1	0.6	<0.5	3.1	9314	0.3	0.3	0.7	349	<1	18	2.45	68	32
Jd-5	0.9	0.6	<0.5	2.9	7746	0.2	0.3	0.9	270	<1	17	2.24	96	75
Jd-6	0.8	0.7	<0.5	3.3	6989	0.4	0.3	1.3	266	<1	17.4	2.21	60	75
Jd-8	0.9	0.7	<0.5	2.2	7820	0.3	0.4	0.9	273	<1	22.3	2.49	89	75
Jd-10	0.8	0.6	<0.5	3	7123	0.3	0.4	1.2	272	<1	18.8	2.41	60	80
Jd-12	0.6	0.6	1.1	3.1	7075	0.2	0.3	0.9	218	<1	17.3	2.18	82	104
Jd-13	0.8	0.5	<0.5	2.3	6862	0.1	0.3	0.8	239	<1	13.9	1.98	65	72
SA-1	0.8	0.9	<0.5	3.8	12565	0.1	0.4	2.3	116	<1	26	2.49	86	210
SA-2	0.2	0.7	<0.5	2.1	7882	0.1	0.3	1.1	93	<1	13.3	1.62	63	58
SA-4	5	0.9	0.7	4.6	2925	0.2	0.5	0.9	2	<1	24.8	2.27	116	338
SA-12	3	1.1	<0.5	5.5	13633	0.2	0.5	2.1	87	1.1	32.1	3.13	69	257
SA-14	6.2	1.2	0.6	8.4	2499	0.2	0.4	1.4	1	<1	26.8	1.95	167	281
SA-15	6	0.7	<0.5	4.5	2704	0.3	0.3	1	3	1.2	13.5	1.46	74	218
NL-1	0.9	0.7	<0.5	4.5	6340	0.3	0.3	1.5	213	<1	22.7	2.56	79	92
NL-4	0.6	0.7	<0.5	2.2	12718	0.1	0.3	0.7	186	<1	18.3	1.93	96	100
NL-5	0.4	0.7	<0.5	2.2	14525	0.1	0.3	0.8	202	<1	19.4	2.07	98	115
NL-7	0.3	0.7	<0.5	1.8	12791	<0.1	0.3	0.7	184	<1	21.9	1.97	94	98
NL-8	1.1	0.7	<0.5	2.3	14531	0.1	0.3	0.8	203	<1	19.9	2.1	93	128
NL-13	1.1	0.7	<0.5	2.5	12771	0.1	0.4	0.7	158	<1	17.1	1.76	87	98
NL-14	0.8	0.7	<0.5	2	13663	<0.1	0.3	0.7	165	<1	16.8	1.73	95	105
NL-15	0.9	0.8	<0.5	2.1	19935	0.2	0.3	0.7	226	<1	19.7	2.05	105	142
NL-18	0.4	1.1	<0.5	4	14739	0.1	0.4	1.2	107	<1	32.1	2.02	127	263
NL-20	0.4	1	<0.5	4	14823	0.1	0.4	1.2	107	<1	25.6	1.95	124	296

10.57647/j.ijes.2025.16895

ing the fractional crystallization as Ti was absorbed by pyroxenes (Ghorbani, 2012). According to (Wilson, 1989), the TiO_2 content is a sensitive indicator of crustal contamination. The Ti depletion in Amol, considering the relatively low degree of partial melting, is likely a result of crustal contamination.

The depletion of P can be attributed to either crustal contamination (Bellieni et al., 1984) or reduction, possibly due to apatite crystallization in the parent magma (Nkouathio et al., 2008; Pearce & Parkinson, 1993).

The depletion of Ba in the trachyte group of this region is likely due to the higher percentage of Na_2O compared to K_2O in this rock group (Figure 3(b)). Ba, which readily reacts with potassium, is not retained in the rock due to the low K_2O content. Ba may have been removed from the environment through hydrothermal solutions (Arghaee, 2017).

The significant depletion of Sr in the trachytes of Amol indicates substantial rock fractionation, possibly due to the crystal fractionation of feldspars in the rift zone (Arghaee, 2017; 2025). It is important to note that fractional crystallization might also lead to the displacement of data points into incorrect ranges (Rollinson & Pease, 2021).

Alkalibasalt (SA1-SA2-SA12): Intraplate basalts typically exhibit a high Zr/Y range (Rollinson & Pease, 2021). An absence of the Y element, as observed in the alkalibasalt samples of Amol, is indicative of intraplate magmatism (Rollinson & Pease, 2021).

The depletion of Nb in alkali basalts is likely a consequence of crustal contamination. As with the trachytes mentioned earlier, the depletion of Sr in alkali basalts can be attributed to the alkaline nature of the primary magma and is related to the crystallization of plagioclase. It is important to note that fractional crystallization can result in the misplacement of data points on diagrams (Arghaee, 2025; Rollinson & Pease, 2021)

Fractional crystallization of most silicate minerals leads to the depletion of Ta and Hf from the melt, while the remaining liquid tends to have high concentrations of Th. Given the significant role of fractional crystallization in the Amol region, Ta depletion is evident in this area (Arghaee, 2017). Ti depletion in alkali basalts of Amol occurs because Ti is easily incorporated into the fractionated phases of basalts, specifically titanomagnetite and pyroxene (Rollinson & Pease, 2021).

4.2.1.2 *JavaherDasht*

The enrichment of Rb, commonly observed in continental rifts, is generally attributed to crustal contamination. The negative Nb anomaly present in many continental rifts and flood basalts can be attributed to two factors: 1) Crustal contamination, and 2) The existence of a residual Nb phase at the source (Cox & Hawkesworth, 1985). A negative anomaly in Nb-Ta (Figure 3(c)) coupled with a positive anomaly in Ba indicates the involvement of crustal elements in the magmatic evolution of these rocks (Taylor & McLennan, 1985).

Studies by (Haghnazar et al., 2008a) suggest that JavaherDasht basalts experienced contamination from the continental crust, demonstrating a significant elemental balance with the lower and middle crust. They argued that the rising magma, originating from the mantle and interacting with the crustal layer, underwent modification, resulting in geochemical changes that falsely mimic the appearance of subduction zones.

4.2.1.3 *South of Lahijan in NarenjLengeh village*

The noticeable increase in the Nb/La ratio observed in these samples is indicative of crustal contamination in the NarenjLengeh basalts, a phenomenon commonly observed in continental rifts and continental flood basalts (Wilson, 1989). A negative Nb anomaly further supports the idea of crustal involvement in the magmatic processes (Rollinson & Pease, 2021).

The depletion of Nb in the continental crust may be attributed to two factors: 1) Nb, like Ti, typically remains in titanite and amphibole minerals within the subducted crust, hindering its entry into the melt during subsequent crustal processes (Hofmann, 1997); 2) Nb is transported primarily by silicate melts and not by subduction solutions (Pearce & Peat, 1995). The rate of Rb depletion in this diagram suggests that crustal contamination in this context differs from that observed in subduction zones, further confirming that this location was not a subduction zone (Figure 3(c)).

The depletion of Nb, P, and Ti indicates that the magma was contaminated by the crust (Li et al., 2016). Meanwhile, there is a rapid decrease from Ce to Lu in the spider diagram (Figure 3(c)), showing some characteristics of rift volcanics (Li et al., 2016; Wang et al., 2006).

Some elements (e.g., Zr, TiO_2, Y, Sc, Ce, and Nb) are largely immobile during the alteration of volcanic rocks owing to metamorphism, hydrothermal events and, weathering (Dagva-Ochira et al., 2020; Floyd & Winchester, 1975). The characteristics of large ion lithophile elements and high field strength elements (Li et al., 2016) of the Cretaceous volcanic rocks in the northern Alborz suggest an affinity to the rift environment.

Continental crust is characterized by enrichment in La rather than Nb (Rezaei et al., 2023; Rudnick & Gao, 2003) and, apart from contributions by lithospheric and asthenospheric mantle, low Nb/La suggest contributions by a crustal contaminant during the evolution of the magma.

4.2.2 *The chondrite-normalized Rare-Earth-Element (REE)*

The chondrite-normalized rare-earth-element (REE) plots for the volcanic rock samples from the northern Alborz exhibit a significant enrichment in light REEs (LREEs) and depletion in heavy REEs (HREEs) (Figure 3(d)).

Notably, a negative Eu anomaly observed in the Amol trachytes indicates the fractional crystallization of plagioclase crystals. In other samples, positive Eu anoma-

10.57647/j.ijes.2025.16895

lies are due to the accumulation of igneous plagioclase during the fractionation of magma in the lower crust (Arghaee, 2025; Rudnick, 1992) or because mantle-derived basalts do not possess a negative Eu anomaly (Tang et al., 2015). The depletion of Sr and Eu can be attributed to the crystalline fractionation of feldspars in rift areas (Ghorbani, 2012). The trace element pattern observed in this diagram closely resembles that observed in alkaline rocks associated with continental rift environments (Beccaluva et al., 2009).

5. Discussions

Many researchers have studied the dynamic evolution of the northern Alborz basalts and other volcanic rocks. According to most reports from our study areas, Cretaceous volcanic rocks in the northern Alborz belong to continental intraplate alkaline volcanism and are associated in space and time with extensional tectonics, specifically with rifting events (Aghazadeh, 2002; Akmali, 2016; Amani et al., 2020; 2021; Arghaee, 2017; 2025; Arghaee et al., 2024; Arghaee & Ghorbani, 2021; 2022a; Delavari et al., 2018; Doroozi et al., 2016; 2015; Haghani & Taki, 2012; Haghnazar, 2009; 2012; Haghnazar & Malakotian, 2009; Haghnazar et al., 2008a; 2015; 2016; 2008b; Jafari Sough et al., 2018; Masoudi & Doroozi, 2014; Moradi, 2017; Taki, 2017). Additionally, some researchers believe that the high volume of Late-Cretaceous volcanic rocks in the northern Alborz is probably related to a significant mantle thermal perturbation associated with asthenosphere upwelling and plume activity (Arghaee, 2017; 2025; Delavari et al., 2018; Namvar, 2018).

Alkaline magmatism is generally associated, in space and time, with extensional tectonics and, more specifically, with rifting events (Fourel et al., 2013; Pirajno, 2015). The petrographic examination of the studied rocks provides evidence of primary magma, indicating the presence of alkaline magma in the region. This evidence was examined in our samples, which include:

A. Alkaline rocks are poor in silica and rich in alkaline elements and rare earth elements, with feldspar and feldspathoid dominating most sections.

B. The presence of stable olivine without corrosion, a characteristic of alkaline series rocks, was observed in our sections.

C. The presence of feldspathoid, such as nepheline and nosean, which are indicators of the alkaline series (Vallipour & Ghodsi, 2009), is present in our samples.

D. In the presence of feldspathoids, orthopyroxene is not formed; therefore, the absence of orthopyroxene in our samples and the presence of clinopyroxene are indicators of the alkaline series, observed in these sections.

E. Due to the rapid eruption of alkaline magma, phenocrysts usually do not have a chance to form. Thus, olivine and feldspathoid are often identified based on the calculation of their norm and are not observed in samples (Ghorbani, 2012). Our samples in the south of Amol often show evidence of rapid magmatism with a lack of phenocrysts (Arghaee, 2017; 2025; Arghaee & Ghorbani, 2021). Normative quartz was not present in the normative mineralogy.

5.1 Interpretation of some geochemical diagrams

In the geochemical studies of CRZ magmas (Continental Rift Zone), the influence of continental crustal contamination must be taken into consideration, as it should in all intraplate magmatic environments (Morgan, 1983).

5.1.1 *Zr/Nb and Y/Nb diagram*

In the Zr/Nb and Y/Nb diagram, the ratios of High Field Strength (HFS) elements, such as Nb and Zr, are crucial indicators. The content of incompatible elements undergoes changes due to fractional crystallization processes, but the ratio between two similar incompatible elements remains constant during fractional crystallization (Jung, 2003). The Zr/Nb ratio has been plotted for the three regions (Figure 5(a)). The graph indicates that the trend of the Zr/Nb ratio is not constant, and there is dispersion in some samples, suggesting that crustal contamination plays a significant role in the studied areas (Wilson, 1989).

However, in south Amol samples, the two groups of alkali basalt and trachyte exhibit a relatively constant ratio (around 5.5 in most samples). This observation suggests that the trachyte magma in Amol was formed through the crystallization of alkali basalt magma.

The high ratio of Zr/Nb and Y/Nb indicates a depleted mantle of Mid-Ocean Ridge Basalt (MORB) origin, whereas a low ratio suggests an origin from an enriched mantle (McDonough & Sun, 1995; Sun & McDonough, 1989) High Zr/Nb ratios, averaging between 5 and 30, indicate derivation from a depleted mantle of P-MORB origin (Sun & McDonough, 1989). The Zr/Nb ratio in NarenjLengeh is 23.96, initially suggesting a tendency towards the depleted mantle. However, in many continental rifts, such as Ethiopia and the Rio Grande, the origin is from a depleted mantle P-MORB. Conversely, a decrease in Zr/Nb indicates an enriched mantle. The average Zr/Nb value in enriched areas of Ocean Island Basalt (OIB) is about 5.8 (Macdonald, 1968; Sun & McDonough, 1989). Amol, with an average of 5.70, indicates an enriched mantle. Specifically, Amol trachytes, with an average of 2.8, show the highest tendency towards an enriched mantle source, while JavaherDasht (8.93) is more inclined towards the enriched mantle source where crustal contamination has played a significant role. The Zr/Nb and Nb/La ratios of mantle-derived melts are 6.3-7.6 and <1.0, respectively; in contrast, those for the crustal-derived melts are 22-25 and <0.46, respectively (Alizadeh et al., 2023; McDonough et al., 1992; Morata et al., 2005).

In enriched OIB samples, the average Y/Nb ratio is about 0.6 (Sun & McDonough, 1989). The average Y/Nb ratio in the depleted mantle is about 12. However, none of the regions reach this number, and their averages include: Amol alkali basalts (1.6), Amol trachytes (0.3), JavaherDasht (1.90), and NarengLengeh (3.5) (Figure 5(b)). Amol trachyte samples with an average Y/Nb of about 0.3 and Zr/Nb of about 5.7 suggest a higher origin from an enriched mantle. Eby (Eby, 1992) proposed that Y/Nb ratios <1.2 and >1.2 indicate mantle and crustal melts, respectively (Alizadeh et al., 2023).

5.1.2 *The Zr/Y and Ti/Y variables diagram*

This diagram is used to distinguish within-plate basalts, especially alkaline types, from other basalt types based on the Zr/Y and Ti/Y variables (Pearce & Gale, 1977). It utilizes the enrichment of Ti and Zr in within-plate basalts (Rollinson & Pease, 2021). Samples from the studied areas fall within the range of within-plate basalts (Figure 5(c)). Within-plate basalts have high Zr/Y ratios, with one of the key indicators of within-plate continental magma being the low enrichment of Y.

5.1.3 *Zr/Nb vs. Y/Nb diagram*

The observed trend, similar to the basalts of the Taos Volcanic Plain in the RioGrande, indicates increased crustal contamination (Dungan et al., 1986) towards the trachytes of Amol, which is consistent with the idea that crustal processes have played a role in influencing the geochemistry of the studied regions (trachytes are shown with dark red in the diagram) (Figure 5(d)).

5.1.4 *Th/Hf diagram and the Zr/Y ratio, plotted against the Zr index*

The tectonic setting of the volcanic rocks in the region, based on the Ta/Hf vs. Th/Hf diagram (Schandl & Gorton, 2002), is related to the within-plate volcanic zone (Figure 4(a)). The Zr/Y ratio, plotted against the Zr index, is an effective tool for distinguishing between Island-arc basalts, Mid-Ocean Ridge Basalts (MORB), and within-plate basalts (Pearce & Norry, 1979). In this diagram, all three studied regions are identified as within-plate basalts (Figure 4(b)). Within-plate basalts typically exhibit high Zr/Y ratios (Rollinson & Pease, 2021).

5.2 Cretaceous Magmatism in the Northern Alborz

Alkaline magmatism and alkali pyroclastic rocks, associated with Jurassic turbidite facies, indicate the onset of a rift system during this period, reaching its peak in the Cretaceous with the emergence of layers of alkaline volcanoes in Northwestern Alborz (Aghanabati, 2004). Our study suggests that this rift likely began east of Alborz in the southern Amol, characterized by alkaline magmatism during the early Cretaceous. Subsequently, this rift expanded further into the northern Alborz. After the deposition of the Tizkoh Formation, pillow lavas were exposed, indicating the formation of the ocean floor post-Tizkoh Formation deposition (Abdolahadi et al., 2025; Akmali, 2016; Arghaee, 2025; Arghaee & Ghorbani, 2022b; Haghnazar et al., 2015; Moradi, 2017; Salehpour et al., 2025). Traces of pillow lavas are visible in the south of Lahijan (Akmali, 2016; Delavari et al., 2018; Moradi, 2017), extending eastward to the south of Chalus (Mousavi, 2003) and Velasht Lake. The geological features continue and are subsequently covered by a large thrust north of Alborz (Hakimi Asiabar et al., 2011).

Upper Cretaceous magmatic activity exhibiting alkaline features and indicative of intraplate tectonics has been extensively documented, particularly in the vicinity of Chalus in western Mazandaran and JavaherDasht regions (Arghaee, 2025; Delavari et al., 2018; Haghnazar, 2009). The peak extensional system occurred in the Late Cretaceous with the substantial development of alkaline volcanic layers (associated with continental rifts) in the western-northern Alborz region (Arghaee & Ghorbani, 2022a; Berberian et al., 1982).

After Campanian, magmatism ceased in Alborz, as evidenced by the absence of normal faults concurrent with sedimentation in these deposits (Arghaee, 2024; Shahidi et al., 2011). These sediments indicate an increase in the depth of sedimentary basins, accompanied by the expansion of marl facies, replacing carbonate facies (Moradi, 2017; Shahidi et al., 2011). Finally, this continental rift was closed by Laramide orogeny (Arghaee, 2025; Doroozi et al., 2015; Masoudi & Doroozi, 2014).

6. Conclusion

In the south of Amol, there is no evidence of magmatic mixing, and the trachytes in this region have formed through the fractional crystallization of parent alkali basaltic magma. Additionally, petrographic evidence in the south of Amol indicates signs of high-temperature, fast-moving lava that originated from depth and exhibits a high oxygen fugacity. Petrographic studies in JavaherDasht and the south of Lahijan, in NarenjLengeh village, reveal evidence of alkaline magmatism due to the presence of nepheline and nosean in trachybasalts and alkali basalts. The presence of lamprophyre dikes with kaersutite hornblende also indicates a primary alkaline magma source in NarenjLengeh.

All geochemical studies are consistent with the petrographic results. In all three studied regions, the analyzed samples fall within the alkaline series, related to the within-plate volcanic zone in the Cretaceous northern Alborz. Geochemical studies, along with a summary of previous studies and field evidence from these areas, reveal a rift system with significant crustal contamination. The consequences of crustal contamination have led to the depletion of TiO_2, Nb, and Zr, altering the interpretation of spider diagrams. Depletion in Nb and Ta is evident in JavaherDasht and NarenjLengeh, as well as in the alkali basalts of Amol. While negative anomalies of Nb and Ti are characteristic of subduction zones, positive anomalies indicate divergent and rift zones. Tran-

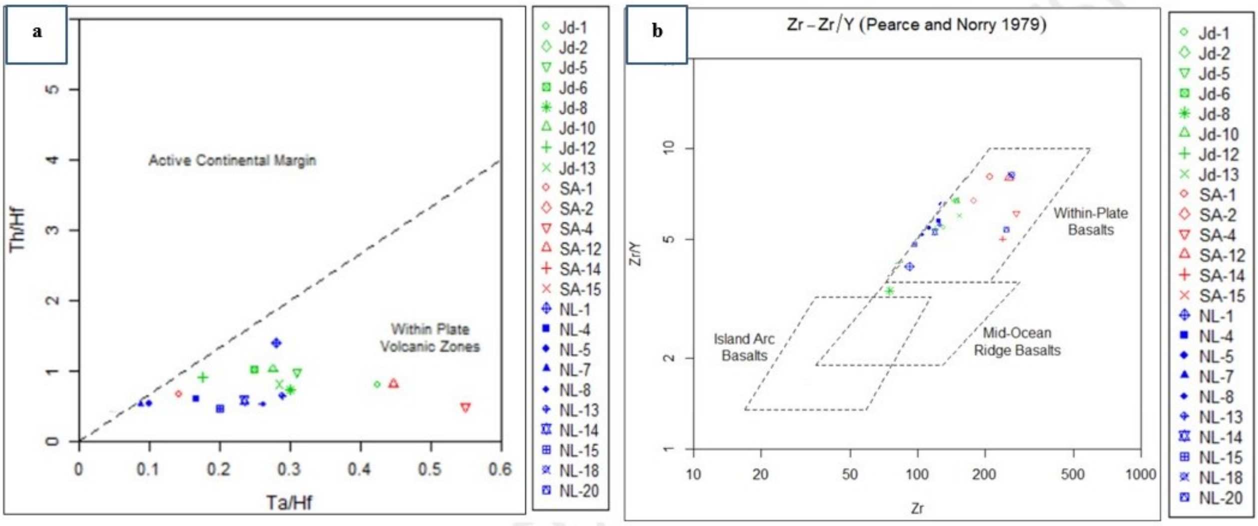

Figure 4. (a) Tectonic setting of the volcanic rocks in the region based on the Ta/Hf vs. Th/Hf diagram (Schandl & Gorton, 2002) (b) Zr/Y ratio plotted against Zr, indicating that all three studied regions are characterized as within-plate basalts (Pearce & Norry, 1979)

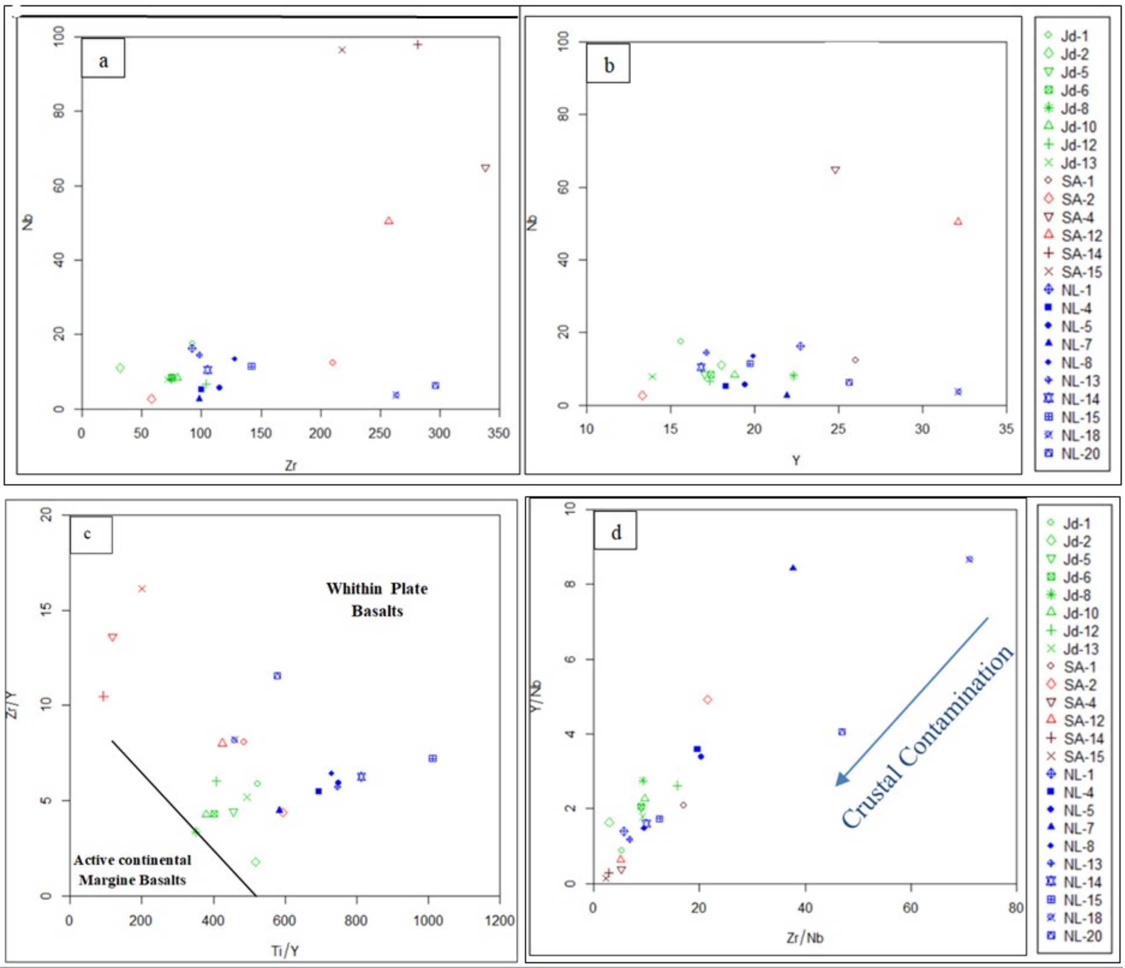

Figure 5. (a) Zr/Nb ratios plotted for the three regions (Wilson, 1989) (b) Y/Nb ratios plotted for the three regions (Sun & McDonough, 1989) (c) The Zr/Y and Ti/Y variables diagram (Pearce & Gale, 1977) (d) Zr/Nb vs Y/Nb diagram (Wilson, 1989)

10.57647/j.ijes.2025.16895

sitional basalts of rift zones, such as the northern Alborz, also exhibit negative anomalies of Ti, Nb, and Ta. Continental crustal contamination can influence these misleading patterns. Fractional crystallization, possibly combined with crustal contamination, is an important process in controlling the geochemical evolution of the region's rift magmas within continental plates.

There is no evidence, such as high K, indicating a subduction environment in the northern Alborz. Specifically, the trachytes of Amol, with their high levels of Nb and Ta, indicate enriched mantle sources. One crucial piece of evidence for intraplate magmatism is the depletion of Y. This characteristic is consistently observed in all studied samples, confirming the intraplate magma origin of the region.

Chondrite-normalized rare-earth-element (REE) plots reveal a notable enrichment in light REEs (LREEs) and depletion in heavy REEs (HREEs). The trace element patterns observed in these diagrams closely resemble those found in alkaline rocks associated with continental rifts. However, it is important to note that there is no evidence of ophiolite complexes in the geological field of this area, and the pillow lava in the NarenjLengeh region is located atop the Shemshak Formation. Considering the absence of vesicles in these samples, it is likely that the depth of water was significant, suggesting that this pillow lava flowed in a deep-water environment in the west of the northern Alborz.

Acknowledgments

This study is based on the PhD thesis of the first author, which was presented at Shahid Beheshti University of Tehran, Iran. We would like to express our appreciation to Dr.José Francisco Santos for providing a postgraduate traineeship in geosciences at the University of Aveiro, Portugal.

Authors contributions

All the authors have participated sufficiently in the intellectual content, conception and design of this work or the analysis and interpretation of the data (when applicable), as well as the writing of the manuscript.

Availability of data and materials

The data that support the findings of this study are available from the corresponding author, upon reasonable request.

Conflict of interests

The author states that there is no conflict of interest.

References

Abdi, A., Khakzad, A., & Vahabzadeh, Q. Alborz cretaceous volcanic basalts with the investigation of rocks from tiran region (amol) [ICMSM01_061, in Persian]. In: In *National conference of mineral sciences*. ICMSM01_061, in Persian. Sari, Iran, 2014. https://doi.org/10.13140/2.1.307056

Abdolahadi, A., Sheikhzakariaee, S. J., Yazdi, A., & Mousavi, S. Z. (2025). Plio-quaternary adakite genesis and post-collisional processes: Whole rock constraints and sr, nd isotopic compositions in alborz magmatic belt, ardabil, iran. *Journal of Mining and Environment*, *16*(2), 737–765. https://doi.org/10.22044/jme.2024.14781.2801

Aghanabati, A. (2004). *Geology of iran* [586 p, in Persian]. Geological Survey of Iran.

Aghazadeh, M. (2002). *Petrological investigation of cretaceous igneous rocks of chalus-marzan abad area (central alborz)* [Master's thesis, Research Institute for Earth Sciences, Geological Survey of Iran] [Master's thesis, in Persian].

Akmali, S. (2016). *Petrology of cretaceous volcano-sedimentary rocks in natash-kuh district in the eastern deylaman area, eastern gilan* [Master's thesis, Imam Khomeini International University, Faculty of Sciences] [Master's thesis, in Persian].

Akmali, S., Asiabanha, A., & Haghnazar, S. (2019). Cretaceous magmatic evolution in the deylaman igneous complex, alborz zone, iran: Change from extensional to compressional regime. *Geological Quarterly*, *63*(4), 757–770. https://doi.org/10.7306/gq.1500

Alavi, M. (1991). Sedimentary and structural characteristics of the paleo-tethys remnants in northeastern iran. *Geological Society of America Bulletin*, *103*, 983–992. https://doi.org/10.1130/0016-7606(1991)103<0983:SASCOT>2.3.CO;2

Alizadeh, E., Li, H., Babazadeh, S. H., Ma, C. H., & Förster, M. W. (2023). Late eocene slab retreat, extension, and mantle upwelling inferred from mantle signatures in potassium-rich magmatism in ne iran. *International Geology Review*, *65*(9), 1586–1600. https://doi.org/10.1080/00206814.2023.2185823

Allen, M., Ghassemi, M. R., Shahrabi, M., & Qorashi, M. (2003). Accommodation of late cenozoic oblique shortening in the alborz range, northern iran. *Journal of Structural Geology*, *25*(5), 659–672. https://doi.org/10.1016/S0191-8141(02)00064-0

Amani, K. H., Delavari, M., Amini, S., & Tabbakh Shabani, A. (2020). The late-cretaceous volcanic rocks from talesh area (western alborz): Chemical variation, crystallization condition, hygrometry and tectonic setting [11th Year, No. 41, pp. 29-52, in Persian]. *Petrology*. https://doi.org/10.22108/ijp.2019.117648.1140

Amani, K. H., Delavari, M., Amini, S., & Tabbakh Shabani, A. (2021). Late cretaceous alkaline basalts of the talesh area: Implication for the tectonic evolution of continental margin in southern eurasia (western alborz) [In Persian]. *Kharazmi Journal of Earth Sciences*, *7*, 39–62. https://doi.org/http://gnf.khu.ac.ir/article-1-2783-en.html

Anders, E., & Grevesse, N. (1989). Abundances of the elements: Meteoric and solar. *Geochimica et Cosmochimica Acta*, *53*(1), 197–214. https://doi.org/10.1016/0016-7037(89)90286-X

Annells, R. N., Arthurton, R. S., Bazley, R. A., & Davies, R. G. (1975). *Explanatory text of the qazvin and rasht quadrangles map: 1:250000*. Geological Survey of Iran.

Arghaee, R. (2017). *Investigation of cretaceous basalt in the south of amol and their relationship with the cretaceous basalt in deccan* [Master's thesis, Shahid Beheshti University, Faculty of Earth Sciences] [Master's thesis, in Persian].

Arghaee, R. Interpreting eruption dynamics and lava placement in cretaceous basaltic lavas of northern alborz: A geological field approach [In Persian]. In: In *42st national geosciences congress*. In Persian. 2024. https://doi.org/10.13140/2.1963808

Arghaee, R. (2025). *The petrogenesis and geodynamics of cretaceous volcanic rocks in the northern alborz and their relationship with mantle plumes* [Doctoral dissertation, Shahid Beheshti University of Iran, Faculty of Earth Sciences, Geology Department] [In Persian].

Arghaee, R., Bento dos Santos, T., Santos, J. F., Ghorbani, M., & Arghaei, S. H. (2024). Mineral chemistry of cretaceous basaltic rocks in the northern alborz, north of iran. *Journal of Pars Arian Territories*, *1*(3), 1–22. https://doi.org/10.61186/jpat.2024.3.5

Arghaee, R., & Ghorbani, M. The interpretation of cretaceous basalts and associated volcanic rocks in the south of amol based on petrographic evidence [In Persian]. In: In *24th symposium of geological society of iran*. In Persian. 2021.

Arghaee, R., & Ghorbani, M. The interpretation of cretaceous pillow lavas in narenjlengeh village in south of lahijan [ISC: 20224-01220, In Persian]. In: In *2nd national biennial conference on geology of the alborz orogen & caspian sea*. ISC: 20224-01220, In Persian. 2022.

Arghaee, R., & Ghorbani, M. The petrography of cretaceous basalts and lamprophyres in narenjlengeh village in south of lahijan [ISC: 20224-01220, In Persian]. In: In *2nd national biennial conference on geology of the alborz orogen & caspian sea*. ISC: 20224-01220, In Persian. 2022.

Arian, M. A., Bazoobandi, M. H., & Elmi, R. (2016). Petrogenesis of volcanic rocks in alasht, mazandaran, iran. *Open Journal of Geology*, *6*, 131–145. https://doi.org/10.4236/ojg.2016.63013

Arjmandzadeh, R., Rashvanlou, V. S., Dabiri, R., & Almasi, A. (2017). Satellite thermal surveys to detect hidden active faults and fault termination: Case study of quchan fault, ne iran. *Iranian Journal of Earth Sciences*, *9*(1), 39–47. https://doi.org/https://oiccpress.com/ijes/article/view/5794

Baharfiruzi, K. H., & Shafeii, R. (2003). Javaherdeh geological map, scale 1:100000.

Ballever, M., LeGoff, E., & Hebert, R. (2001). The tectothermal evolution of the caledonian belt of northern brittany, france: A neoproterozoic volcanic arc. *Tectonophysics*, *33*, 119–143. https://doi.org/10.1016/s0040-1951(00)00234-1

Beccaluva, L., Bianchini, G., Natali, C., & Siena, F. (2009). Continental flood basalts and mantle plumes: A case study of the northern ethiopian plateau. *Journal of Petrology*, *50*(7), 1377–1403. https://doi.org/10.1093/petrology/egp024

Bellieni, G., Comin-Chiaramonti, P., Marques, L. S., Melfi, A. J., Piccirillo, E. M., Nardy, A. J. R., & Roisenberg, A. (1984). High and low-ti flood basalts from the paraná plateau (brazil): Petrology and geochemical aspects bearing on their mantle origin. *Neues Jahrbuch für Mineralogie, Abhandlungen*, *150*, 272–306.

Berberian, F., Muir, I. D., Pankhurst, R. J., & Berberian, M. (1982). Late cretaceous and early miocene andean-type plutonic activity in northern makran and central iran. *Journal of the Geological Society*, *139*(5), 605–614. https://doi.org/10.1144/gsjgs.139.5.0605

Berberian, M. (1983). *Structural evolution of the iranian plateau; contribution to the seismotectonics of iran, part iv: Continental deformation in the iranian plateau* (tech. rep. No. Report 52). Geological Survey of Iran.

Berberian, M., & King, G. C. (1981). Towards a paleogeography and tectonic evolution of iran. *Canadian Journal of Earth Sciences*, *18*, 210–265. https://doi.org/10.1139/e81-019

Best, M. (2003). *Igneous and metamorphic petrology* (2nd ed.). Blackwell Publishing. https://doi.org/10.1017/S0016756805360432

Bucher, K., & Grapes, R. (2011). *Petrogenesis of metamorphic rocks* (8th ed.). Springer. https://doi.org/10.1007/978-3-031-12595-9

Chatterjee, N., & Bhattacharji, S. (2008). Trace element variations in deccan basalts: Roles of mantle melting, fractional crystallization and crustal assimilation. *Journal of the Geological Society of India*, *71*, 171–188.

Cox, K. J., & Hawkesworth, C. J. (1985). Geochemical stratigraphy of the deccan traps at mahabaleshwar, western ghats, india, with implications for open system magmatic processes. *Journal of Petrology*, *26*, 355–377. https://doi.org/10.1093/petrology/26.2.355

Dabiri, R., Akbari-Mogaddam, M., & Ghaffari, M. (2018a). Geochemical evolution and petrogenesis of the eocene kashmar granitoid rocks, ne iran: Implications for fractional crystallization and crustal contamination processes. *Iranian Journal of Earth Sciences*, *10*(2), 68–77. https://doi.org/https://oiccpress.com/ijes/article/view/5628

Dabiri, R., Hagdoust, H., & Arjmandzadeh, R. (2018b). Geochemical distribution of heavy metals and assessment of environmental indicators in chah-shaljami polymetal ore deposit, south of birjand, iran. *Geopersia*, *8*(2), 307–317. https://doi.org/10.22059/geope.2018.260186.648395

Dagva-Ochira, L., Oyunchimeg, T. U., Enkhdalai, B., Safonova, I., Li, H., Otgonbaatar, D., Soh Tamehea, L., & Sharav, D. (2020). Middle paleozoic intermediate-mafic rocks of the tsoroidog uul' accretionary complex, central mongolia: Petrogenesis and tectonic implications. *Lithos*, *376–377*, 105795. https://doi.org/10.1016/j.lithos.2020.105795

Delavari, M., Moradi, R., & Tabbakh Shabani, A. (2018). Mineral chemistry, thermobarometry and tectonomagmatic setting of late-cretaceous volcanic rocks from the kojid area (south of lahijan, northern alborz). *Petrology*, *9*(33). https://doi.org/10.22108/ijp.2017.104651.1033

Doroozi, R., Vaccaro, C., & Masoudi, F. (2016). Rhonite in undersaturated alkaline gabbroic rocks, central alborz, north iran: Petrography and mineral chemistry. *Arabian Journal of Geosciences*, *9*(15). https://doi.org/10.1007/s12517-016-2684-3

Doroozi, R., Vaccaro, C., Masoudi, F., & Petrini, R. (2015). Cretaceous alkaline volcanism in south marzanabad, northern central alborz, iran: Geochemistry and petrogenesis. *Geoscience Frontiers*, *7*, 937–951. https://doi.org/10.1016/j.gsf.2015.11.004

Dungan, M. A., Lindstrom, M. M., McMillan, N. J., Moorbath, S., Hoefs, J., & Haskin, L. A. (1986). Open system magmatic evolution of the taos plateau volcanic field, northern new mexico: 1. the petrology and geochemistry of the servilleta basalt. *Journal of Geophysical Research: Solid Earth*, *91*(B6), 5999–6028. https://doi.org/10.1029/JB091iB06p05999

Eby, G. N. (1992). Chemical subdivision of the a-type granitoids: Petrogenetic and tectonic implications. *Geology*, *20*(7), 641–644. https://doi.org/10.1130/0091-7613(1992)020<0641:CSOTAT>2.3.CO;2

Floyd, P. A., & Winchester, J. A. (1975). Magma type and tectonic setting discrimination using immobile elements. *Earth and Planetary Science Letters*, *27*, 211–218. https://doi.org/10.1016/0012-821X(75)90031-X

Fourel, L., Milelli, L., Jaupart, C., & Limare, A. (2013). Generation of continental rifts, basins, and swells by lithosphere instabilities. *Journal of Geophysical Research: Solid Earth*, *118*. https://doi.org/10.1002/jgrb.50218

Ghasempour, M. R., Ghazi, J. M., Biabangard, H., & Dabiri, R. (2014). Petrogenetic evolution of plio-quaternary mafic lavas in nehbandan (east iran). *Iranian Journal of Earth Sciences*, *6*(2), 133–141. https://doi.org/https://sanad.iau.ir/Journal/ijes/Article/917225

Ghorbani, M. (2012). *Advanced petrography and petrogenesis of igneous rocks*. Pars Arian Zamin Publications.

Ghorbani, M. (2013). *Economic geology of iran: Mineral deposits and natural resources*. Springer. https://doi.org/10.1007/978-94-007-5625-0

Ghorbani, M. (2021). *The geology of iran: Tectonic, magmatism and metamorphism*. Springer. https://doi.org/10.1007/978-3-030-71109-2

Guest, B., Axen, G. J., Lam, P. S., & Hassanzadeh, J. (2006). Late cenozoic shortening in the west-central alborz mountains, northern iran, by combined conjugate strikeslip and thin-skinned deformation. *Geosphere*, *2*, 35–52. https://doi.org/10.1130/GES00019.1

Haghani, M., & Taki, S. Petrogenesis of belde volcanic rocks located in the south of noor city (mazandaran province). In: In *Iran's first applied geochemistry conference*. 2012.

Haghnazar, S. H. (2009). *Petrology of mafic rocks in javaherdasht area, east of gilan province* [Doctoral dissertation, Shahid Beheshti University].

Haghnazar, S. H. (2011). Petrology of basaltic dykes in upper jurassic-lower cretaceous limestones in javaherdasht area, western central alborz. *Journal of Earth & Resources, Islamic Azad University of Lahijan*, *4*.

Haghnazar, S. H. (2012). Petrology, geochemistry and tectonic setting of javaherdasht cretaceous gabbro, north alborz. *Petrological Journal*, *10*, 79–94.

Haghnazar, S. H., & Malakotian, S. (2009). Petrography and geochemistry of javaherdasht basalts: Crystal fractionation and crustal contamination. *Iranian Journal of Crystallography and Mineralogy*, *17*(2), 253–266.

Haghnazar, S. H., Malakotian, S., & Allahyari, K. (2011). Petrological, mineralogical and geochemical properties of javaherdasht gabbros. *Iranian Journal of Crystallography and Mineralogy*, *18*(4), 545–562.

Haghnazar, S. H., Malakotian, S., Allahyari, K., & Taki, S. (2008a). Petrographical, geochemical and isotopical evidence of crustal contamination in javaherdasht basalts. *Journal of Tarbiat Moalem University of Science*, *8*(3).

10.57647/j.ijes.2025.16895

Haghnazar, S. H., Malakotian, S., & Allahyari, K. H. (2015). Tectono-magmatic setting of cretaceous pillow basalts in the north part of the alborz mountains in east of gilan province (north of iran): A part of ophiolite sequence or intracontinental rift? [in Persian]. *Scientific Quarterly Journal of Geosciences*, *24*(94), 171–182. https://doi.org/10.22071/gsj.2015.42908

Haghnazar, S. H., Shafeie, Z., & Sharghy, Z. (2016). Petrogenesis and tectonic setting of a basalt-trachyte-rhyolite suite in the spilli area (south of siahkal), north of iran: Evidence of continental rift-related bimodal magmatism in alborz [in Persian]. *Petrological Journal*, *7*(27), 43–60. https://doi.org/10.22108/ijp.2016.21017

Haghnazar, S. H., Vosoughi Abedini, M., & Pourmoafi, M. (2008b). Mantle source characteristics of javaherdasht basalts (east of gilan), based on geochemical and isotopic features [in Persian]. *Iranian Journal of Geology*, *2*(8). https://doi.org/https://www.magiran.com/p747379

Hakimi Asiabar, S., Pourkermani, M., Shahryari, S., Ghorbani, M., & Ghasemi, M. (2011). Geological zones of western alborz mountains [in Persian]. *Journal of Basic Sciences of Islamic Azad University*, (81). https://doi.org/https://sid.ir/paper/70254/en

Hofmann, A. M. (1997). Mantle geochemistry: The message from oceanic volcanism. *Nature*, *385*, 219–229. https://doi.org/10.1038/385219a0

Jackson, J., Priestley, K., Allen, M., & Berberian, M. (2002). Active tectonics of the south caspian basin. *Geophysical Journal International*, *148*(2), 214–245. https://doi.org/10.1046/j.1365-246X.2002.01588.x

Jafari Sough, R., Asiabanha, A., & Nasrabadi, M. (2018). Geochemistry of cretaceous hydromagmatic lava flows in separdeh district, ne qazvin, central alborz [in Persian]. *Iranian Journal of Crystallography and Mineralogy*, *26*, 717–732. https://doi.org/10.29252/ijcm.26.3.717

Johannsen, A. (1931). *A descriptive petrography of the igneous rocks* (Vol. 40). University of Chicago.

Jung, C. (2003). *Geochemical and isotope geochemical investigations on tertian volcanites of the hocheifel* [PhD thesis]. Philipps University of Marburg.

Juteau, T., & Maury, R. (1999). *The oceanic crust, from accretion to mantle recycling*. Springer-Praxis.

Kananian, A., Salvati, M., Esmaili, D., & Asibanha, A. (2004). Mineral chemistry of clinopyroxene in amlash igneous rocks (north of iran) [in Persian]. *Journal of Science, University of Tehran*, *30*(2), 229–245. https://doi.org/https://sid.ir/paper/2236/en

Khan Nasr Esfahani, A. (2012). Tectonic setting of metabasites of the neo-tethyan oceanic remains in sanandaj-sirjan structural zone, west of isfahan. *Iranian Journal of Earth Sciences*, *4*(2), 75–84. https://doi.org/https://sanad.iau.ir/Journal/ijes/Article/917189

Lan, Z., Huyskens, M., Le Hir, G., Mitchell, R., Yin, Q. Z., Zhang, G., & Li, X. H. (2022). Massive volcanism may have foreshortened the marinoan snowball earth. *Geophysical Research Letters*, *49*, e2021GL097156. https://doi.org/10.1029/2021GL097156

Le Bas, M. J., Le Maitre, R. W., Streckeisen, A., & Zanettin, B. (1986). A chemical classification of volcanic rocks based on the total alkali-silica diagram. *Journal of Petrology*, *27*, 745–750. https://doi.org/10.1093/petrology/27.3.745

Li, H., Xi, X. S., Sun, H. S., Kong, H., Wu, Q. H., Wu, C. M., & Gabo-Ratio, J. A. S. (2016). Geochemistry of the batang group in the zhaokalong area, yushu, qinghai. *Acta Geologica Sinica*, *90*, 704–721. https://doi.org/10.1111/1755-6724.12699

Macdonald, G. A. (1968). Composition and origin of hawaii lavas. *Geological Society of America Memoirs*, *116*, 477–522. https://doi.org/10.1130/MEM116-p477

Malaekeh, A., Ghasemi, M. R., Afzal, P., & Solgi, A. (2021). Fractal modeling and relationship between thrust faults and carbonate-hosted pb-zn mineralization in alborz mountains, northern iran. *Geochemistry*, *81*(4), 125803. https://doi.org/10.1016/j.chemer.2021.125803

Masoudi, F., & Doroozi, R. (2014). Study of fractionation trend in south marzan abad basic volcanic rocks based on geochemical models [in Persian]. *Scientific Journal of Kharazmi University*, *13*(4), 919–936. https://doi.org/http://jsci.khu.ac.ir/article-1-1557-en.html

McDonough, W. F., & Sun, S. S. (1995). The composition of the earth. *Chemical Geology*, *120*, 223–253. https://doi.org/10.1016/0009-2541(94)00140-4

McDonough, W. F., Sun, S. S., Ringwood, A. E., Jagoutz, E., & Hofmann, A. W. (1992). Potassium, rubidium, and cesium in the earth and moon and the evolution of the mantle of the earth. *Geochimica et Cosmochimica Acta*, *56*(3), 1001–1012. https://doi.org/10.1016/0016-7037(92)90043-I

Middlemost, E. A. K. (1972). A simple classification of volcanic rocks. *Bulletin of Volcanology*, *36*(2), 382–397. https://doi.org/10.1007/BF02596878

Mollai, H., Dabiri, R., Torshizian, H. A., Pe-Piper, G., & Wang, W. E. (2021). Upper neoproterozoic garnet-bearing granites in the zeber-kuh region from east central iran micro plate: Implications for the magmatic evolution in the northern margin of gondwanaland. *Geologica Carpathica*, *72*(6), 461–481. https://doi.org/10.31577/GeolCarp.72.6.2

Monsef, I., Zhang, Z., Shabanian, E., le Roux, P., & Rahgoshay, M. (2022). Tethyan subduction and cretaceous rift magmatism at the southern margin of eurasia: Evidence for crustal evolution of the south caspian basin. *Earth-Science Reviews*, 104012. https://doi.org/10.1016/j.earscirev.2022.104012

Moradi, R. (2017). *Geochemistry and petrogenesis of the cretaceous volcanic rocks in kojid area, northern alborz* [Master's thesis, Kharazmi University, Faculty of Earth Sciences] [Master's thesis, in Persian].

Morata, D., Oliva, C., Cruz, D. R., & Suarez, M. (2005). The bandurrias gabbro; late oligocene alkaline magmatism in the patagonian cordillera. *Journal of South American Earth Sciences*, *18*(2), 147–162. https://doi.org/10.1016/j.jsames.2004.09.001

Morgan, M. (1983). Constraints on rift thermal processes from heat flow and uplift. *Tectonophysics*, *94*, 277–298. https://doi.org/10.1016/0040-1951(83)90021-5

Morse, S. A. (1980). *Basalt and phase diagrams: An introduction to the quantitative use of phase diagrams in igneous petrology*. Springer-Verlag. https://doi.org/10.1007/978-1-4612-6081-3

Mousavi, R. (2003). *Petrology of late cretaceous igneous rocks of javaherdeh with special emphasis on navdis lodge volcanics* [Master's thesis, Geological Survey of Iran] [Master's thesis, in Persian].

Namvar, R. (2018). *Geochemical features of cretaceous volcanism in north damavand and its application in alborz tectono-magmatic evolution* [Master's thesis, Kharazmi University, Faculty of Earth Sciences] [Master's thesis, in Persian].

National Geoscience Database of Iran. (n.d.). Ngdir [Accessed 2025].

Nazari, H., Omrani, J., Shahidi, A., Salamati, R., & Moosavi, A. (2004). Geological map of anzali, 1:100000 [Sheet D3e5864, Geological Survey of Iran].

Nazari, M., Arian, M. A., Solgi, A., Zareisahamieh, R., & Yazdi, A. (2023). Geochemistry and tectonomagmatic environment of eocene volcanic rocks in southeastern abhar, nw iran. *Iranian Journal of Earth Sciences*, *15*(4), 228–247. https://doi.org/10.30495/ijes.2023.1956689.1746

Nelson, S. T., & Montana, A. (1992). Sieve-textured plagioclase in volcanic rocks produced by rapid decompression. *American Mineralogist*, *77*, 1242–1249.

Nkouathio, D. G., Kagou Dongmo, A., Bardintzeff, J. M., Wandji, P., Bellon, H., & Pouclet, A. (2008). Evolution of volcanism in graben and horst structures along the cenozoic cameroon line. *Mineralogy and Petrology*, *94*, 287–303. https://doi.org/10.1007/s00710-008-0018-1

Ousta, S. h., Ashja-Ardalan, A., Yazdi, A., Dabiri, R., & Arian, M. A. (2024). Petrogenesis and tectonic implications of miocene dikes in se bam (iran). *Geopersia*, *14*(1), 89–111. https://doi.org/10.22059/geope.2023.364334.648729

Pearce, J. A., & Gale, G. H. Identification of ore-deposition environment from trace-element geochemistry of igneous host rocks. In: In *Volcanic processes in ore genesis*. Vol. 7. Geological Society Special Publications. 1977, pp. 14–24. https://doi.org/10.1144/GSL.SP.1977.007.01.03

Pearce, J. A., & Norry, M. J. (1979). Petrogenetic implications of ti, zr, y and nb variations in intrusive rocks. *Contributions to Mineralogy and Petrology*, *69*, 33–47. https://doi.org/10.1007/BF00375192

Pearce, J. A., & Parkinson, I. J. Trace element models for mantle melting: Application to volcanic arc petrogenesis. In: In *Geological society special publications*. Vol. 76. 1993, pp. 373–403. https://doi.org/10.1144/GSL.SP.1993.076.01.19

Pearce, J. A., & Peat, D. W. (1995). Tectonic implications of the composition of volcanic arc magmas. *Annual Review of Earth and Planetary Sciences*, *23*, 251–285. https://doi.org/10.1146/annurev.ea.23.050195.001343

Philpotts, A. R., & Ague, J. J. (2009). *Principles of igneous and metamorphic petrology* (2nd ed.). Cambridge University Press. https://doi.org/10.1017/CBO9780511813429

Pirajno, F. (2015). Intracontinental anorogenic alkaline magmatism and carbonatites associated mineral systems and the mantle plume connection. *Gondwana Research*, *27*, 1181–1216. https://doi.org/10.1016/j.gr.2014.09.008

Rajabi, A., Rastad, E., & Canet, C. (2013). Metallogeny of permian–triassic carbonate hosted zn–pb and f deposits of iran: A review for future mineral exploration. *Australian Journal of Earth Sciences*, *60*(2), 197–216. https://doi.org/10.1080/08120099.2012.754792

Rezaei, L., Moazzen, M., & Timmerman, M. (2020). Geochemistry and clinopyroxene mineral chemistry of basalts in the gasht-masuleh area, alborz mountains. *Iranian Journal of Crystallography and Mineralogy*, *28*(3), 609–622. https://doi.org/10.29252/ijcm.28.3.609

Rezaei, L., Timmerman, M. J., Moazzen, M., Altenberger, U., Sláma, J., Sudo, M., Günter, C., Wilke, F. D. H., & Schleicher, A. M. (2023). Mid-cretaceous extensional magmatism in the alborz mountains, north iran; geochemistry and geochronology of gasht-masuleh gabbros. *Swiss Journal of Geosciences*, *116*, 14. https://doi.org/10.1186/s00015-023-00443-2

10.57647/j.ijes.2025.16895

Rollinson, H., & Pease, V. (2021). *Using geochemical data to understand geological processes*. Cambridge University Press. https://doi.org/10.1017/9781108777834

Rudnick, R., & Gao, S. (2003). Composition of the continental crust. *Treatise on Geochemistry*, *3*, 1–64. https://doi.org/10.1016/B0-08-043751-6/03016-4

Rudnick, R. L. (1992). Restites, eu anomalies, and the lower continental crust. *Geochimica et Cosmochimica Acta*, *56*(3), 963–970. https://doi.org/10.1016/0016-7037(92)90040-P

Salavati, M. (2008). Petrology, geochemistry and mineral chemistry of extrusive alkalic rocks of the southern caspian sea ophiolite, northern albroz, iran. *Journal of Applied Sciences*, *8*(12), 2202–2216. https://doi.org/10.3923/jas.2008.2202.2216

Salavati, M., Kananian, A., Samadi Soofi, A., & Zaeimnia, F. (2009). Mineral chemistry of ultramafic rocks from the southern caspian sea ophiolite (eastern gilan): Evidence for high-pressure crystal fractionation. *Iranian Journal of Crystallography and Mineralogy*, *17*(1), 1–20. https://doi.org/10.1020_370b3b4f1640104ae2c5e00edce70d64.pdf

Salavati, M., & Samadissofi, A. (2008). Geochemical petrology study of basalts in the south of amlesh region (east of gilan). *Lahijan Department of Earth and Resources Scientific Research Quarterly*, 29–38.

Salehpour, S., Arian, M. A., Rad, A. J., Zarei Sahamieh, R., & Yazdi, A. (2025). Geochemistry and technomagmatic environment of eocene volcanic rocks in yuzbashi chay region, west of qazvin (iran). *Iranian Journal of Earth Sciences*, *17*(1), 1–13. https://doi.org/10.57647/j.ijes.2025.1701.04

Schandl, E. S., & Gorton, M. P. (2002). Application of high field strength elements to discriminate tectonic settings in vms environments. *Economic Geology*, *97*(3), 629–642. https://doi.org/10.2113/gsecongeo.97.3.629

Sengor, A. M. A new model for the late paleozoic-mesozoic tectonic evolution of iran and implications for oman. In: In *The geology and tectonics of the oman region*. Vol. 49. Geological Society Special Publications, 1990, pp. 797–831. https://doi.org/10.1144/GSL.SP.1992.049.01.49

Sengor, A. M., Altiner, D., Cin, A., Ustaomer, T., & Hsu, K. J. Origin and assembly of the tethyside orogenic collage at the expense of gondwanaland. In: In *Gondwana and tethys*. Vol. 37. 1988, pp. 119–181. https://doi.org/10.1144/GSL.SP.1988.037.01.09

Shahidi, A., Barrier, E., Brunet, M. F., & Saidi, A. (2011). Tectonic evolution of the alborz in mesozoic and cenozoic. *Scientific Quarterly Journal of Geosciences*, *21*(81), 201–216. https://doi.org/10.22071/gsj.2011.54384

Stampfli, G. M. (1996). The intra-alpine terrain: A paleotethyan remnant in the alpine variscides. *Eclogae Geologicae Helvetiae*, *89*(1), 13–42.

Stampfli, G. M., Marcoux, J., & Baud, A. (1991). Tethyan margins in space and time. *Palaeogeography, Palaeoclimatology, Palaeoecology*, *87*, 373–409. https://doi.org/10.1016/0031-0182(91)90142-E

Stocklin, J. Northern iran: Alborz mountains. In: In *Mesozoic cenozoic orogenic belts*. Vol. 4. Geological Society Special Publication, 1974, pp. 213–234. https://doi.org/10.1144/GSL.SP.2005.004.01.12

Stocklin, J. Possible ancient continental margin in iran. In: In *The geology of continental margins*. Springer, 1974, pp. 873–887. https://doi.org/10.1007/978-3-662-01141-6_64

Sun, S. S., & McDonough, W. F. Chemical and isotopic systematics of oceanic basalts: Implications for mantle composition and processes. In: In *Geological society special publications*. Vol. 42. 1989, pp. 313–345. https://doi.org/10.1144/GSL.SP.1989.042.01.19

Taki, S. (2017). The role of fractional crystallization in the evolution of magma of the upper cretaceous volcanic and subvolcanic rocks from the nageleh sar syncline. *Iranian Journal of Crystallography and Mineralogy*, *25*(3), 501–512. https://doi.org/10.18869/acadpub.ijcm.25.3.501

Talebian Borojenie, H., Sheykhzakariaei, S. J., Dabiri, R., & Yazdi, A. (2025). Petrogenesis and tectonic implications of neoproterozoic to cenozoic a-type granitoids in nw iran: Geochemical and tectonic constraints. *Iranian Journal of Earth Sciences*.

Tang, M., Rudnick, R. L., McDonough, W. F., Gaschnig, R. M., & Huang, Y. (2015). Europium anomalies constrain the mass of recycled lower continental crust. *Geology*, *43*(8), 703–706.

Taylor, S. R., & McLennan, S. M. (1985). The continental crust: Its composition and evolution.

Teknik, V., & Ghods, A. (2017). Depth of magnetic basement in iran based on fractal spectral analysis of aeromagnetic data. *Geophysical Journal International*, *209*(3), 1878–1891.

Vahdati Daneshmand, F. (1991). Geological map of amol quadrangle scale 1:250,000.

Vallipour, M., & Ghodsi, J. (2009). *Petrography and atlas of igneous rocks* [(in Persian)]. Islamic Azad University of Mashhad Publications.

Vasigh, Y., Darvishzadeh, A., Vosoughi Abedini, M., & Emam, i. M. (2014). Petrology of heiran area submarine lavas in north east of ardebil a case study of caspian sea southern margin geosuture [(in Persian)]. *Scientific Quarterly Journal, Geosciences*, *24*(93). https://doi.org/https://doi.org/10.22071/gsj.2014.43536

Verdel, C., Wernicke, B. P., Hassanzadeh, J., & Guest, B. (2011). A paleogene extensional arc flare-up in iran. *Tectonics*, *30*, TC300. https://doi.org/https://doi.org/10.1029/2010TC002809

Wang, X., Gao, S., Liu, X., Yuan, H., Hu, Z., Zhang, H., & Wang, X. U. (2006). Geochemistry of high-mg andesites from the early cretaceous yixian formation, western liaoning: Implications for lower crustal delamination and sr/y variations. *SCI CHINA SER D*, *49*, 904–914. https://doi.org/https://doi.org/10.1007/s11430-006-2016-7

Wilson, M. (1989). *Igneous petrogenesis a global tectonic approach*. Uniwin Hyman, London. https://doi.org/https://doi.org/10.1007/978-1-4020-6788-4

Wilson, M., Downes, H., & Cebria, J. (1995). Contrasting fractionation trends in coexisting continental alkaline magma series; cantal, massif central, france. *Journal of Petrology*, *36*, 1729–1753.

Yazdi, A., ShahHoseini, E., & Razavi, R. (2016). Ams, a method for determining magma flow in dykes (case study: Andesite dyke). *Research Journal of Applied Sciences*, *11*(3), 62–67. https://doi.org/http://doi.org/10.3923/rjasci.2016.62.67

Yazdi, A., Shahhosseini, E., & Moharami, F. (2022). Petrology and tectono-magmatic environment of the volcanic rocks of west torud–iran. *Iranian Journal of Earth Sciences*, *14*(1), 40–57. https://doi.org/https://doi.org/10.30495/ijes.2022.1929200.1601

Zaeimnia, F., Kananiyan, A., Samadi, R., & Salvati, M. Origin of south amlash alkaline gabbros, north of iran [(in Persian)]. In: In *12th symposium of geological society of iran*. (in Persian). 2008.

Zanchi, A., Berra, F., Mattei, M., Ghassemi, M. R., & Sabouri, J. (2006). Inversion tectonics in central alborz, iran. *Journal of Structural Geology*, *28*(11), 2023–2037. https://doi.org/https://doi.org/10.1016/j.jsg.2006.06.020

Zanchi, A., Zanchetta, S., Berra, F., Mattei, M., Garzanti, E., Molyneux, S., Nawab, A., & Sabouri, J. (2009). The eo-cimmerian (late? triassic) orogeny in north iran. *Geological Society of London, Special Publications*, *312*, 31–55. https://doi.org/https://doi.org/10.1144/SP312.3